Carbon Research

Analytical methods, molecular structures and biogeochemical behaviors of dissolved black carbon

Yalan Chen[1], Ke Sun[1*] , Zhibo Wang[1], Enyao Zhang[1], Yan Yang[1] and Baoshan Xing[2]

Abstract

Dissolved black carbon (DBC) is one of the most active fractions in the black carbon (BC) continuum and plays a significant role in the global dissolved organic matter (DOM) pool. Connecting the BC pool between territorial and marine environments, the biogeochemical processes of DBC are significant for many aspects of aquatic chemistry. Once entering the aquatic environment, DBC will undergo degradation and exert continuing effects on water ecology. DBC can change the migration and transport of pollutants and affect associated microbial communities. Therefore, the knowledge of the fate and transport of DBC is of great importance. In this work, the molecular structures of different DBC were examined and summarized to provide a basis for understanding the environmental processes of DBC. Current research progress on the photodegradation of DBC, interactions between DBC and microorganisms, and the effects of DBC on the fate and transport of contaminants were critically reviewed. The qualitative and quantitative analytical methods for DBC were assessed in detail. To date, the environmental behaviors of DBC are far from fully understood in part due to the lack of systematic methods. Compared with the relatively well-studied photodegradation of DBC, microbial transformation of DBC is poorly understood. Moreover, DBC is exposed to continuous light illumination and microbial metabolization, thus the combined effects of photodegradation and biodegradation are crucial to the cycling and turnover of DBC in aquatic environment and deserve further investigations. In addition, research on the sorption processes, redox reactions and DBC-assisted photo-transformations of contaminants is still at its emerging stages.

Article Highlights

• The qualitative and quantitative analytical methods for dissolved black carbon (DBC) were discussed.

• The structural characteristics of DBC and its difference from natural dissolved organic matter were summarized.

• The photodegradation and biodegradation of DBC, and its interaction with pollutants were reviewed.

Keywords: Dissolved black carbon, Analytical method, Chemical structure, Photo-transformation, Biodegradation, Pollutants

*Correspondence: sunke@bnu.edu.cn

[1] State Key Laboratory of Water Environment Simulation, School of Environment, Beijing Normal University, Beijing 100875, China
Full list of author information is available at the end of the article

Graphical Abstract
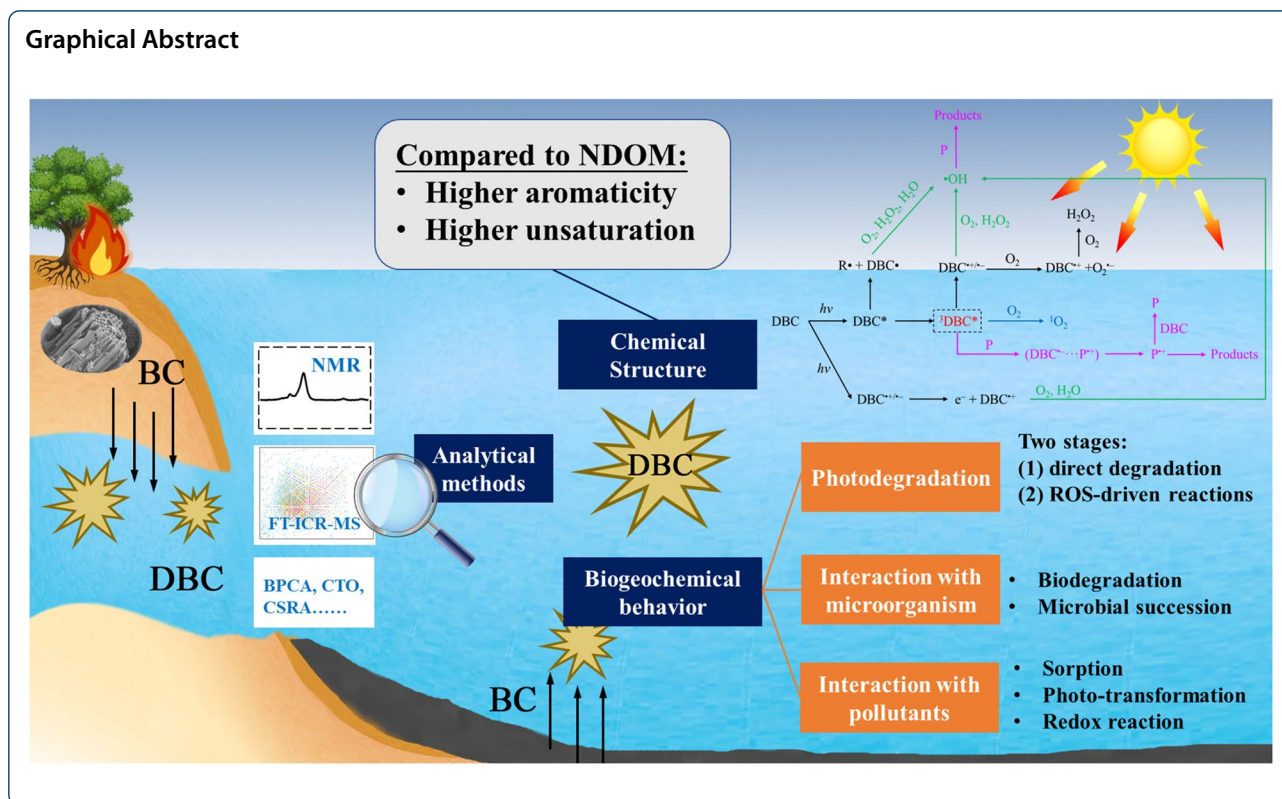
1 Introduction

Fossil fuel combustion, forest fires, and biochar application have led to large amounts of black carbon (BC) entering the natural environment (Coppola et al., 2019). BC is heterogeneous in nature and ranges from slightly charred fractions to highly condensed aromatic components formed through incomplete combustion at high temperatures. It is estimated that approximately 60 Pg of BC has been produced by landscape fires since 1750 (Jones et al., 2019). On a global scale, biomass burning and fossil fuel combustion are expected to produce 114–383 Tg yr^{-1} and 2–29 Tg yr^{-1} of BC (Coppola et al., 2019), respectively. Owing to the large quantities and recalcitrant nature of this carbon-rich material (Masiello and Druffel, 1998; Preston and Schmidt, 2006; Reisser et al., 2016), BC represents a significant but previously ignored carbon pool in the global carbon budget (Jones et al., 2019; Woolf et al., 2010).

In the current review, dissolved black carbon (DBC) is defined as the water-soluble fraction (generally refers to fraction of <0.45 μm) extracted from BC. DBC is one of the most labile and mobile fractions in the BC continuum (Wang et al., 2013), and it can easily be released via soil infiltration and surface runoff. Globally, DBC represents approximately 10% of the global fluxes of dissolved organic matter (DOM) from rivers to oceans (Jaffe et al., 2013),

which is a significant pathway for BC emission to the sea. Moreover, the fact that more than 2% of oceanic DOM exerts a heat-induced molecular signature also suggests a considerable DBC fluxes from land to oceans (Dittmar and Paeng, 2009; Jaffe et al., 2013; Mannino and Rodger Harvey, 2004). As such, the biogeochemical behaviors of DBC may be particularly significant in regulating greenhouse gas emissions and stabilizing organic matter.

The molecular structures of DBC are the basis for understanding their biogeochemical behaviors. However, due to the varied parent solids (e.g., biomass types) and formation conditions (e.g., production temperature) and the heterogeneous nature of BC (Alan Roebuck et al., 2017), the molecular structures of different DBC vary greatly (Bostick et al., 2020). The diversity, complexity and heterogeneity of DBC make the prediction of their environmental behaviors and effects complicated. Once DBC enters the environment, it will inevitably undergo various environmental processes. Photodegradation is one of the most important pathways for DBC transformation and is also a relatively well-studied process (Fu et al., 2016). DBC contains many aromatic structures, and it may be one of the more photoactive fractions in the DOM pool (Fu et al., 2016). Biodegradation is another important pathway for DBC transformation. Although recalcitrant in nature, DBC can be utilized by microbes via co-metabolism of other

Chen *et al. Carbon Research*   (2022) 1:23

Page 3 of 19

labile carbon source (Qi et al., 2020). In contrast, DBC, as a refractory carbon source, may also affect the constitution and succession of microbial communities (Hockaday et al., 2006; Zhou et al., 2021). Similar to well-studied DOM, DBC can affect the fate and transport of pollutants via sorption processes, redox reactions or radical-driven processes (Fu et al., 2016; Smith et al., 2013). However, the understanding of the aforementioned environmental behaviors of DBC is still far from robust, which is partly attributed to the lack of a well-organized analytical system.

In this work, qualitative and quantitative analytical methods for DBC were discussed in detail. In addition, the research on the molecular structures and environmental behaviors (e.g., photodegradation, interaction with microorganisms and pollutants) of different DBC was critically reviewed. The current knowledge gaps and future perspectives were put forward. This work can be useful for future studies on the environmental behaviors and effects of DBC.

1.1 Analytical methods for DBC

Until now, information regarding the environmental behaviors of DBC in aquatic environments has been far from robust, which is in part due to the lack of a well-recognized and consensus method. Recent studies have gradually uncovered the photodegradation of DBC under specified laboratory conditions. However, DBC in real aquatic environments is far more complicated as it is well-dispersed in the natural DOM (NDOM) pool. The lack of consensus regarding standard separation and quantification methods results in considerable uncertainties on the sources and fates of DBC in natural aquatic systems. The combined utilization of advanced technologies can help improve our understanding of the environmental transformations of DBC.

1.1.1 Chemothermal oxidation (CTO) method

At present, CTO is popular for isolating BC from environmental samples (Gustafsson et al., 2001; Zencak et al., 2007), and it can similarly determine the abundance of DBC in the DOM pool (Qi et al., 2020). The quantitative principle of the CTO method is based on the determination of the highly condensed aromatic components in DBC. First, the environmental DOM sample is extracted using ultrafiltration/lyophilization (Mannino and Rodger Harvey, 2004) and solid-phase extraction (Wang et al., 2016; Xu et al., 2016). Carbonate is removed by chemical pretreatment. The recovered DOM sample is thermally oxidized at 375 °C for 2 h to remove the non-DBC DOM. Then, the residue is oxidized again at 850 °C for 2 h, and the DBC abundance is determined by the resultant CO_2 generated during this process. Several reports have shown that DBC concentrations in river and oceanic waters determined by the CTO method resemble those determined by the benzene polycarboxylic acid method (Coppola et al., 2018; Dittmar and Koch, 2006; Dittmar et al., 2012b; Wagner et al., 2019; Wang et al., 2016), indicating that CTO is a potentially efficient quantitative method. In addition, Qi et al. (2020) excluded the possibility of additional DBC generation from DOM during thermal oxidation at 375 °C, which further confirmed the accuracy of measured CTO results. However, questions remain for DBC of relatively low production temperature (e.g., 450 °C), which contained abundant non-condensed components but very little residues for CTO determination (Hammes et al., 2007; Nguyen et al., 2004). Another deficiency concerns the positive bias due to the samples charring during the analysis (Hammes et al., 2007). Thus, influencing factors and the effects of environmental matrix should be considered when applying this method (Wagner et al., 2018).

1.1.2 Benzene polycarboxylic acid (BPCA) method

The BPCA method is another quantification analytical method that was originally applied to determine the abundance of BC in soil environments. The quantitative principle of the BPCA method is based on the detection of polysubstituted benzene carboxylic acids containing 3–6 carboxylic acid groups (B3CA, B4CA, B5CA, and B6CA, respectively), which are converted by thermochemically oxidizing condensed aromatic compounds (Dittmar, 2008; Schneider et al., 2010; Ziolkowski et al., 2011). The distribution patterns of polysubstituted benzene carboxylic acids appropriately indicate the condensed aromaticity of BC and DBC. The BPCA aromatic condensation index, which represents the average number of carboxyl groups in DOM, is usually used as an indicator of condensed aromatic cluster sizes (Bostick et al., 2018; Ziolkowski and Druffel, 2010).

Glaser et al. (1998) first developed the BPCA method and employed it to measure artificially produced BC. Hockaday et al. (2007) used the BPCA method to track the export of BC in DOM from soils. Dittmar (2008) then optimized the oxidation temperature and duration of the BPCA method and successfully applied it to determine both the concentration and the structural properties of DBC. The BPCA method gradually became the primary DBC quantification technology, and was widely applied to track DBC in river (Stubbins et al., 2015), stream (Ding et al., 2013; Jaffé et al., 2012), and marine waters (Coppola and Druffel, 2016), as well as to investigate the photochemistry (Stubbins et al., 2012b) and biochemistry (Bostick et al., 2021) of DBC. For example, Stubbins et al. (2012b) quantified oceanic DBC using benzene polycarboxylic acid markers and found that DBC was more photolabile than colored DOM. Bostick et al. (2021) further

Chen *et al. Carbon Research*   (2022) 1:23

Page 4 of 19

found that photodegradation and biodegradation altered the BPCA composition of BC leachates. Specifically, photodegradation process profoundly removed high-substituted B5CA and B6CA, whereas biodegradation process promoted the loss of low-substituted B3CA and B4CA. Liu et al. (2022) compared the photodegradation patterns of DBC and NDOM released from composted Rice Straw. They observed a much higher yields of B3CA, B4CA, B5CA, and B6CA from DBC (2.81 mg C/L) than NDOM (0.43 mg C/L). The photodegradation process decreased the abundance of all polysubstituted benzene carboxylic acids, with larger losses of high-substituted B5CA (50.28%) and B6CA (51.51%) relative to the low-substituted B3CA (34.04%) and B4CA (42.45%). This indicated a more significant removal of high-condensed aromatic carbon in DBC, which was consistent with FT-ICR-MS results. Such results demonstrated that biogeochemical processing may play a significant role in reworking the BPCA composition of DBC. Moreover, distinct differences were noted for the BPCA compositions of BC solid and corresponding DBC. Therefore, although the BPCA composition can be utilized to distinguish different DOM pools, the mismatch of BPCA composition between DBC and parent solid, as well as the dynamically changing BPCA distribution of DBC after irradiation or microbial reworking, suggest the uncertainty of BPCA method in assessing the source of DBC.

1.1.3 Compound-specific radiocarbon analysis (CSRA)

Compared to BPCA method, CSRA is an efficient technique for dating and tracing sources of DBC. This analytical method mainly includes two steps: 1) oxidizing DBC into BPCA, as mentioned above, and 2) determining the ^{14}C abundance of BPCA using accelerator mass spectrometry (Wei et al., 2017). Based on the distinctive ^{14}C ages of the DBC produced from biomass burning (modern) and fossil fuel combustion (ancient) (Coppola and Druffel, 2016; Coppola et al., 2018; Masiello and Druffel, 1998; Ziolkowski and Druffel, 2010), the CSRA method can be applied to verify the relative contribution of these two sources. In addition, comparing the distinctive ^{14}C ages between riverine DBC (modern) (Coppola et al., 2018; Wang et al., 2016) and oceanic DBC (ancient, > 20,000 years) (Coppola and Druffel, 2016; Ziolkowski and Druffel, 2010) helps to better elucidate the transport and export of DBC from land to sea, as changes in ^{14}C ages suggest significant contributions from microbial and photochemical degradation processes (Qi et al., 2020). However, limitations remain in BPCA-specific CSRA method, as it is hard to distinguish whether the ^{14}C-depleted DBC result from the contemporary input of pre-aged DBC sources (e.g., fossil fuel

combustion products) or from the in-situ aging of DBC (Coppola and Druffel, 2016).

1.1.4 Fourier transform ion cyclotron resonance mass spectrometry (FT-ICR-MS)

FT-ICR-MS has unsurpassed mass-resolution abilities and can provide molecular-level identification of DBC. The primary competitive advantage of FT-ICR-MS is that it does not require the prior separation of individual molecules before identification (Sleighter and Hatcher, 2007). With ultrahigh mass-resolution spectrometry data, FT-ICR-MS techniques can identify more than 1000 molecules at a time by assigning $C_aH_bN_cO_d$ molecular formulas to each spectral peak. In addition, it can also distinguish between molecules of nearly identical nominal mass (Koch et al., 2007; Kujawinski and Behn, 2006).

To visualize the molecular compositions of DBC, van Krevelen diagrams for CHO and CHON molecules are often applied to describe the types of DBC compounds. The H/C atomic ratio is related to the aromaticity of DBC molecules. To evaluate the bulk composition of DBC, different characteristic parameters have been calculated. The modified aromaticity index (AI_{mod}) can be utilized to determine the bulk aromaticity of DBC, as well as the relative abundance of aliphatic ($AI_{mod} < 0.5$), aromatic ($0.5 < AI_{mod} < 0.67$), and condensed aromatic ($AI_{mod} > 0.67$) molecules (Hao et al., 2018; Osterholz et al., 2016a). In natural environment, molecular formulas of $AI_{mod} > 0.67$ are generally defined as part of the DBC pool (Koch and Dittmar, 2006). The DBE index is applied to analyze the number of double bonds and rings in a molecule, which manifests the degree of unsaturation and aromaticity of DBC molecules (Stenson et al., 2003). The nominal oxygen state of carbon (NOSC) is used to evaluate the degree of oxidation and molecular polarity or hydrophobicity of different components (Riedel et al., 2012).

FT-ICR-MS techniques have also been applied to investigate the shifts in DBC molecular structural compositions under different biogeochemical processes like photodegradation and biodegradation. Stubbins et al. (2010) used FT-ICR-MS to identify DBC in Congo River water and found that the DBC undergoes faster photodegradation than the other structural components of DOM. Ward et al. (2014) found that the condensed aromatics in DBC were preferentially degraded via photooxidation. Latch et al. (2003) determined the conversion of DBC molecules into smaller molecular weights components by the photo-oxidation of the higher molecular weight fractions. As such, FT-ICR-MS showed great advantages in uncovering the molecular change mechanism of DBC during environmental processes. Compared with photodegradation, few studies have focused

Chen *et al. Carbon Research*   (2022) 1:23

Page 5 of 19

on the biogeochemical processes of DBC. Zhou et al. (2021) showed that the successions of microbial communities were closely associated with the aromaticity of DOM on the basis of FT-ICR-MS analysis. Similar to NDOM, the involvement of DBC in the DOM pool can potentially alter the community compositions and functions of microorganisms (Hao et al., 2018). In return, microbial activities can change the molecular structure of DBC (Qi et al., 2020), a phenomenon that lacks supporting evidence from FT-ICR-MS analysis (Chen et al., 2022; Goranov et al., 2022).

As different molecules vary in their ionization efficiencies, the FT-ICR-MS technique is only qualitative or semiquantitative (Kujawinski et al., 2004). To avoid the substantial suppression of analyte signals, solid-phase extraction (SPE) is generally applied to concentrate and desalt DBC samples (Schmidt et al., 2003). Although SPE can guarantee a relatively high recovery rate for DBC (Li et al., 2017), the selective loss of certain compounds, such as biopolymers, CHNO, and CHOP molecules, is inevitable (Chen et al., 2016; Zhang et al., 2021b). Besides, FT-ICR-MS shows poor reproducibility and the commonly used electrospray ionization (ESI) mode is susceptible to interference of solvents and impurities (Enke, 1997). Several studies suggested that ESI mode may not be able to measure large aromatics and condensed aromatics in DBC of high pyrolysis temperature (Wozniak et al., 2020). Also, the ions transportation efficiency depends on the optimization of ion optics, the vacuum state of ion cyclotron resonance cell, and related parameters (Marshall et al., 1998). Additionally, considerable uncertainties exist in selecting one proper formula from the multiple formula assignments. To alleviate this problem, the formula screening can be conducted according to following rules (Liu et al., 2015; Shi et al., 2021; Vetere and Schrader, 2017). In most cases, CHO components were more reliable than CHON components (Herzsprung et al., 2014, 2015). In addition, ESI− mode favors detection of acidic functional groups, while ESI + mode facilitates the measurement of CHON, CHONS, amines and amino sugars (Lin et al., 2012; Ohno et al., 2016; Sleighter and Hatcher, 2007). Moreover, FT-ICR-MS technology is one of the most expensive and time-consuming methods, which partly limits its widespread use (Dittmar and Koch, 2006). It should be noted that the combined application of multiple techniques can help to alleviate the deficiency of a single method. BPCA and FT-ICR-MS can reflect similar reactivity patterns of DBC (e.g., the preferential photodegradation of B5CA and B6CA by BPCA (Stubbins et al., 2012b) corresponding with the condensed aromatic structures by FT-ICR-MS (Stubbins et al., 2010)), thus complementing each other (Liu et al., 2022). Also, solid-state ^{13}C nuclear magnetic resonance shows good

potential in quantitative investigations of DBC structures, and the combination of ^{13}C NMR and FT-ICR-MS makes it possible to determine the condensed aromatic structures containing nitrogen and sulfur (Abdul Jameel et al., 2019; Helms et al., 2015; Hertkorn et al., 2016; Li et al., 2015; Porto et al., 2019). Several studies have used ^{13}C NMR to quantify the structural changes in DBC derived from different parent solids and to compare their functional constituents with NDOM (Huang et al., 2021; Tian et al., 2019). Fu et al. (2016) first applied ^{13}C NMR to distinguish the structural changes in DBC under photoirradiation and observed major decreases in aromatic and methyl peaks after irradiation. Other techniques, such as GC–MS, can be applied for qualitative assessments of less aromatic DBC and used as supplementary tools for the accurate determination of possible molecules. For example, Hao et al. (2018) used GC–MS to verify the potential molecules identified via FT-ICR-MS and found the concentrations of specific molecules as a function of their hydrothermal carbonization temperatures, suggesting the potential of GC–MS to uncover structural changes in DBC. However, GC–MS are restricted to volatile organic compounds with low molecular weights, and they cannot identify polar organic compounds with high molecular weights. As a result, the information for more than 90% of DBC molecules is lost.

1.2 Chemical and molecular structures of DBC
Owing to the varied organic matter sources and formation processes, the chemical and structural properties of DBC significantly differ from those of well-studied NDOM. Herein, we summarized the structural characteristics of DBC, which is a crucial basis for understanding its environmental behavior.

1.2.1 Optical spectral characteristics of DBC
DBC derived from different parent solids exhibits various UV–Vis spectral features. Several studies have suggested that DBC released from bamboo biochar exhibits broad, featureless, and declining spectral characteristics, which are similar to those of humic substances (Chen et al., 2002; Qu et al., 2016; Wei et al., 2017). Fu et al. (2016) and Bostick et al. (2020) also showed featureless UV–vis spectra for DBC released from bamboo and oak biochars generated at 650 °C. However, DBC released from oak biochars generated at 400 °C (Bostick et al., 2020) and bamboo hydrochars (Hao et al., 2018) displayed characteristic absorption peaks. Some spectral parameters were applied to indirectly infer the structural characteristics of the DBC. It is generally acknowledged that DBC is more aromatic than NDOM, as indicated by SUVA$_{254}$ values. Fu et al. (2016) concluded that DBC may have smaller molecular weights than DOM, as the E_2/E_3 parameters

Chen *et al. Carbon Research* (2022) 1:23

Page 6 of 19

for DBC (5.47) were higher than those of commonly studied DOM (3.06 ~ 4.77) (Fu et al., 2016). However, some studies have shown that the E_2/E_3 values of NDOM may exceed 8.6 (Helms et al., 2008), while those of DBC may be as low as 1.7 ~ 2.9 (Bostick et al., 2020). Such results may drive a widely divergent conclusion. Thus, the information provided by UV–vis is still limited, and comparisons between different studies are constrained. In addition, owing to the disparities in DBC sources, no unanimous conclusions about DBC spectral characteristics can be reached, at least for the time being.

Three-dimensional fluorescence (EEM) spectra can be used as an indicator of DBC component characteristics. Table 1 summarizes the diverse fluorescence peaks and corresponding components of DBC. In general, DBC produced at higher temperatures has simpler EEM spectra. In addition, the EEM spectra of DBC are simpler than those of NDOM, as the latter often contain several peaks in different EEM regions (Chen et al., 2003). To obtain more compositional information about DBC, EEM-PARAFAC has become increasingly popular (Chen et al., 2020; Han et al., 2021; Yamashita et al., 2021). However, this method requires large sample quantities, and the effectiveness of component separation is hard to guarantee. Moreover, the comparison of PARAFAC model between different studies is hard. One useful solution is to upload the PARAFAC model to the OpenFluor online software (Murphy et al., 2014), which facilitates the searching of the similar components reported in previous records.

1.2.2 Chemical structures of DBC
NDOM are mainly composed of aliphatic structures (> 50%), as indicated by ^{13}C NMR analysis (Fig. 1). Owing to the intensive dehydration and condensation reactions during thermal treatment, both biochar- and hydrochar-derived DBC generally possess more abundant aromatic structures but fewer aliphatic structures than NDOM. Typically, hydrochar-derived DBC contains more aliphatic structures than biochar-derived DBC does. In addition, biochar-derived DBC is also more abundant in carboxy or aldehyde functional groups than NDOM, while hydrochar-derived DBC barely contains these structures. As the parent material's thermal maturity increases, the proportions of aromatic and alkyl components in biochar-derived DBC increase, while those of oxygenated functional groups decrease (Bostick et al., 2018). With respect to hydrochar-derived DBC, the proportion of O-alkyl structures, aromatic C-O and aldehyde decrease, while those of carboxyl and aromatic C increase (Hao et al., 2018). This summary confirmed the higher aromaticity of DBC than NDOM and further suggested

that pyrolysis technique can produce more aromatic structure than hydrothermal carbonization treatment.

1.2.3 Molecular structural characteristics of DBC
With respect to molecular structures, DBC is generally composed of condensed aromatic compounds, aliphatic hydrocarbons, thermally treated biopolymer oligomers, and low molecular weight components (Bostick et al., 2018; Fu et al., 2016). As indicated by Fig. 2a, the average molecular weights of different DOM follow a decreasing order of biochar-derived DBC, riverine NDOM and hydrochar-derived DBC. In addition, biochar-derived DBC exhibits higher double bond equivalents (DBEs), O/C ratios and AI_{mod} but lower H/C ratios than riverine NDOM (Fig. 2b–e). As the production temperature increases, the molecular structures of DBC shift to lower molecular weights (Hao et al., 2018). The molecular diversity and H/C ratios of biochar-derived DBC decrease, while the O/C ratios and DBE increase (Huang et al., 2021). For hydrochar-derived DBC, however, higher production temperatures often lead to higher molecular diversity (Hao et al., 2018). When the temperature exceeds a certain limit, however, the molecular diversity may exhibit a slight decrease, which can be potentially attributed to the repolymerization of small organic compounds (Hao et al., 2018).

Although the chemical properties of DBC vary with the solid structures of the parent material (e.g., biomass type and production parameters), the common aromatic characteristics of DBC can be used as a marker for their content in environmental samples. Kim et al. (2004) first applied FT-ICR-MS to identify the structural characteristics of DBC in aqueous environments. The differentiation of DBC in environmental DOM samples is based on the consistency of their molecular elemental compositions (H/C < 1) with solid BC (0.27 < H/C < 1.3) and their differences from NDOM (H/C > 1). In addition, DBE characteristics are also applied to distinguish DBC (DBE/C > 1) from NDOM. Some studies also used the BPCA method to differentiate DBC in environmental DOM samples (Mori et al., 2021). The distinction was based on the fact that DBC molecules contain a higher average quantity of aromatic rings (> 7) (Dittmar and Koch, 2006) than NDOM (< 5) (Hockaday et al., 2007).

1.3 Environmental behaviors of DBC
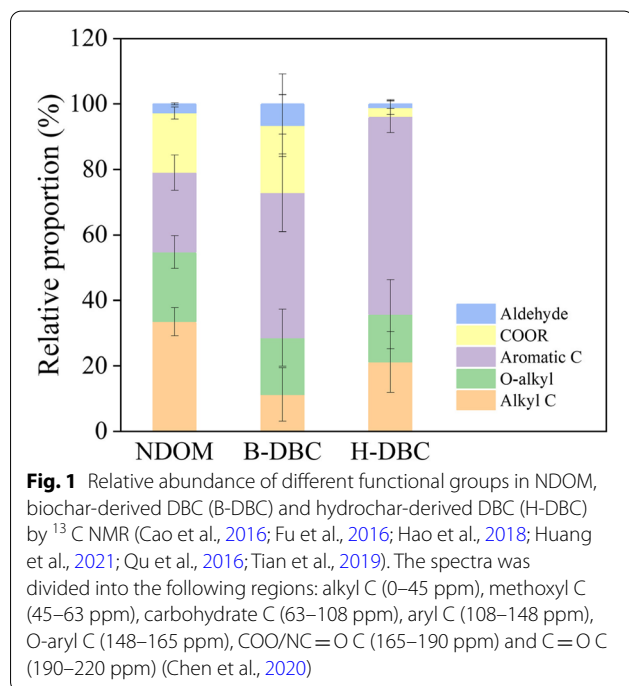#### 1.3.1 Photochemical degradation of DBC
DBC is acknowledged as one of the more photoactive components in the DOM pool (Fu et al., 2016; Stubbins et al., 2012b), and its photodegradation rate may far exceed that of colored DOM (Stubbins et al., 2012b). It has been estimated that the photochemical half-life of oceanic DBC is less than 800 years, far below its

Chen *et al. Carbon Research*   (2022) 1:23

Page 7 of 19

Table 1 Fluorescence peaks and corresponding components of DBC derived from BC of different biomass types and generated at different production temperatures

Biomass	Production temperature (°C)	Ex (nm)	Em (nm)	Correponding component	References
Feedstock-derived NDOM					
Maize straw	–	350	440	Humic acid-like	(Zhang et al., 2020b)
		240	460	Fulvic acid-like	
Pig manure	–	350	450	Humic acid-like	
		240	500	Fulvic acid-like	
Spartina alterniflora	–	220	340	Aromatic protein	(Chen et al., 2020)
		270	340	Typtophan	
Pig manure	–	250	420	Fulvic acid	
		320	430	Humic acid-like	
		220	350	Aromatic protein	
		275	350	Typtophan	
Biochar-derived DBC					
Bamboo	400	320	420	Humic acid-like	(Fu et al., 2016)
Tealeaf willow, feather moss	452	245	415	Fulvic acid-like	(Ward et al., 2014)
		305	415	Humic acid-like	
Oak	400	275	340	tryptophan-like	(Bostick et al., 2020)
		330, 266	400	Pyrene-like	
	650	330, 266	400	Pyrene-like	
Pinewood sawdust	300	260	330	Tryptophan	(Han et al., 2021)
		280	410	Humic acid-like	
	400, 500	300	420	Humic acid-like	
		250	420	Humic acid-like	
Bamboo sawdust	300	260	325	Tryptophan	
		280	400	Tryptophan & protein-like	
	400	300	420	Humic acid-like	
		240	420	Hydrophobic acid	
	500	ND	ND	ND	
Corncob	300	280	420	Humic acid-like	
		230	420	Hydrophobic acid	
	400	300	420	Humic acid-like	
		240	410	Fulvic acid-like	
	500	260	400	Humic acid-like	
Corn straw	300	300	420	Humic acid-like	
		240	420	Hydrophobic acid	
	400	280	410	Humic acid-like	
		250	420	Hydrophobic acid	
	500	250	400	Fulvic acid-like	
Maize straw	300	320	445	Humic acid-like	(Zhang et al., 2020b)
		240	450	Fulvic acid-like	
	500	250	400	Hydrophobic acid	
Pig manure	300, 500	330	420	Humic acid-like	
		230	450	Fulvic acid-like	
Hydrochar-derived DBC					
Bamboo	180, 210	260	330	Typtophan	(Hao et al., 2018)
	240	250	310	Tyrosine- & protein-like	
		280	300	Tyrosine- & protein-like	
	270, 300, 330	260	330	Typtophan	
		280	330	Protein-like containing typtophan	

Table 1 (continued)

Biomass	Production temperature (°C)	Ex (nm)	Em (nm)	Correponding component	References
Spartina alterniflora	210–260	270	350	Typtophan	(Chen et al., 2020)
		225	340	Aromatic protein	
Pig manure	210–260	320	400	Humic acid-like	
		225	400	Hydrophobic acid	

Fig. 1 Relative abundance of different functional groups in NDOM, biochar-derived DBC (B-DBC) and hydrochar-derived DBC (H-DBC) by ^{13} C NMR (Cao et al., 2016; Fu et al., 2016; Hao et al., 2018; Huang et al., 2021; Qu et al., 2016; Tian et al., 2019). The spectra was divided into the following regions: alkyl C (0–45 ppm), methoxyl C (45–63 ppm), carbohydrate C (63–108 ppm), aryl C (108–148 ppm), O-aryl C (148–165 ppm), COO/NC=O C (165–190 ppm) and C=O C (190–220 ppm) (Chen et al., 2020)

previously assumed apparent age of 1,500 years (Stubbins et al., 2012b). As such, photochemical degradation may be one of the significant pathways for DBC mineralization and alteration in surface waters (Fu et al., 2016; Stubbins et al., 2012b, 2010; Wagner et al., 2018; Ward et al., 2014).

There are two different stages of DBC photodegradation (Bostick et al., 2020). The most photoactive fractions are lost in the initial 2 days and roughly correspond to the aryl-C by ^{1}H NMR and condensed aromatic carbons (ConACs) by the BPCA and FT-ICR-MS method (Bostick et al., 2020; Yan et al., 2022). The less photolabile fraction of non-condensed components (small aromatic compounds, aliphatic compounds including low-molecular-weight acids, and alcohols), however, is likely to be photo-mineralized by radical-driven propagation reactions generated by the mineralization of aromatic components (Fig. 3). These results indicated that photo-mineralization may be chemically selective and act on different photoactive components with the extension

of irradiation time. Moreover, the carbon loss sequence of DBC produced at different temperatures varied with photoirradiation time. Yan et al. (2022) reported that the mineralization ratio of 300 °C DBC was higher than that of 450 °C DBC during 24 h of photoirradiation. Chen et al. (2022) also showed that 300 and 450 °C DBC degraded faster than 650 °C DBC after 24 h of irradiation. Bostick et al. (2020) showed that the photodegradation ratios of 250 and 525 °C DBC were higher than those of 400 and 650 °C during the initial 24 h, respectively, while those of 525 and 650 °C DBC were still higher than those of 250 and 400 °C DBC. Such results indicated that the photodegradation pattern of DBC was quite complex during the first stage, potentially attributed to the heterogeneous reactivity of different subcomponents in DBC. After a long period of photoirradiation, however, a similar pattern that the mineralization ratio of DBC increased with production temperature was observed in different studies (Bostick et al., 2020; Yan et al., 2022), suggesting the overall higher photolability of DBC produced at higher temperatures. However, due to the use of different feedstock for DBC production and the application of varied illumination intensity, the photodegradation pattern of DBC was still largely unknown.

Photodegradation processes have a preference for specific components, such as the chromophoric fractions and aromatic substances. Many studies have reported a rapid decrease in the fluorescence peak intensity of EEM spectra (Bostick et al., 2020; Fu et al., 2016), indicating that fluorescent DBC fractions are highly susceptible to light irradiation. Bostick et al. (2020) further pointed out that some fluorescent components are especially photolabile. For example, humic acid-like fluorescent compounds were particularly susceptible to loss, and their degradation ratio was even higher than that of less condensed fulvic acid-like fluorescent compounds. Aromatic components have also been acknowledged as photoactive fractions in DBC, but their half-lives are longer than those of the fluorescent fractions (Fu et al., 2016). Stubbins et al. (2010) first reported direct evidence for the photodegradation of DBC like molecules in Congo River and showed that more than 90% of aromatic compounds potentially associated with BC were lost based on FT-ICR-MS. Ward et al. (2014) also revealed a nearly
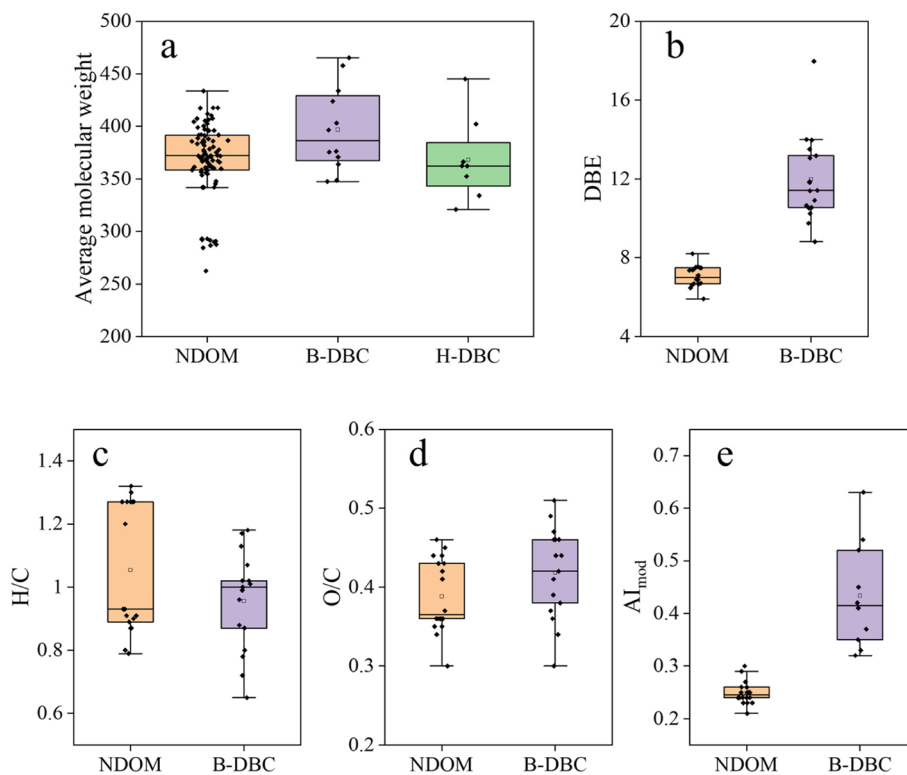
Fig. 2 Differences in the molecular structures, including a) average molecular weight, b) DBE, c) H/C atomic ratio, d) O/C atomic ratio and e) AI_{mod}, between riverine NDOM, biochar-derived DBC (B-DBC) and hydrochar-derived DBC (H-DBC) by FT-ICR-MS (Chen et al., 2022; Hao et al., 2018; Huang et al., 2020, 2021; Seidel et al., 2014; Stubbins et al., 2010; Wagner et al., 2015; Ward et al., 2014; Yan et al., 2022)
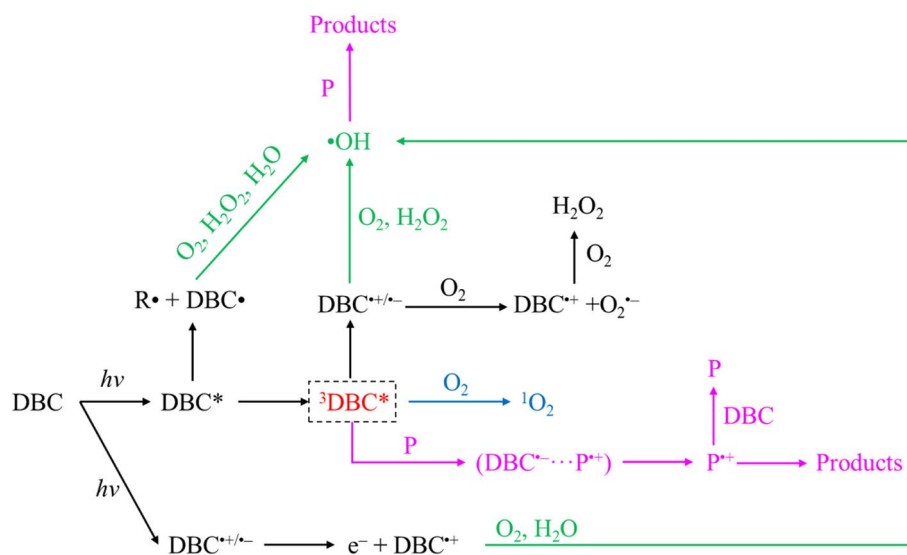

Fig. 3 Pathways for reactive species generation from DBC under photoirradiation and potential photo-transformation mechanisms of pollutants mediated by DBC. P represents pollutants

Chen *et al. Carbon Research* (2022) 1:23

Page 10 of 19

complete loss of aromatic compounds in DBC after 17 h of sunlight irradiation. Several studies also observed major losses in benzene polycarboxylic acids after irradiation and suggested that ConACs have especially poor photo-resistance (Liu et al., 2022; Spencer et al., 2009; Stubbins et al., 2012a, 2012b). Given that the $SUVA_{254}$ value is linearly correlated with the aromatic content by ^{13}C NMR (Weishaar et al., 2003), the decrease in $SUVA_{254}$ during irradiation observed in previous studies also suggests a major loss of the aromatic components of DBC (Bostick et al., 2020). In addition to aromatic components, photo-transformation also preferentially targets aliphatic hydrocarbons containing methyl functional groups (Fu et al., 2016), as well as polysubstituted olefinic moieties (Goranov et al., 2020). However, Yan et al. (2022) suggested the removal of condensed aromatics and carbohydrate in DBC during photoirradiation, while Chen et al. (2022) reported the photo-mineralization of lignin-like components. The mismatch may be due to the use of different feedstock types for DBC production and the varied intensities of photobleaching treatments.

During irradiation, the molecular diversity and average molecular weights of DBC show a decreasing trend (Chen et al., 2022; Stubbins et al., 2010; Wagner and Jaffé, 2015; Yan et al., 2022). The apparent photo-induced transformation in DBC relative abundance from higher molecular weight fractions to lower molecular fractions can be attributed to the combined processes of complete mineralization to CO_2 and structural photo-alteration (Wagner and Jaffé, 2015). The photo-transformation of DBC was dominated by photo-oxidation (>68%), with photo-mineralization contributing only approximately 8 ~ 13% as the subsidiary reaction (Ward et al., 2014). On the one hand, the selective removal of DBC with higher molecular weights and the preservation and generation of DBC with lower molecular weights by irradiation may generate a secondary DBC pool with potentially enhanced bioavailability (Bruun et al., 2008). Also, the lower molecular weight fractions may exhibit priming effects on DBC biodegradation (Woods et al., 2010). On the other hand, some of the biolabile subcomponents in DBC can also be degraded under photoirradiation (Bittar et al., 2015). Thus, the mixing effects by photodegradation and biodegradation processes may significantly alter the turnover rate of DBC and merit further investigation.

DBC structure may be one of the most important factors influencing its photolability. Although several studies have revealed the varied ConAC content in DBC from different sources (Bostick et al., 2018; Fu et al., 2016; Norwood et al., 2013; Ward et al., 2014), few studies have investigated their corresponding photolability. Bostick et al. (2020) compared the photolability of DBC derived from oak biochars at different charring temperatures and found that DBC produced at higher temperatures was more photoactive than that at lower temperatures. Our recent work also supported this result (Yan et al., 2022). Beyond charring temperature, the effects of other factors, such as biomass type (e.g., livestock manure with high protein and traditional lignocellulosic biomass), deserve further investigation.

Exposure to sunlight can also enhance the release of DBC from its parent solid. Previous studies have shown that the photo-dissolution of particulate organic matter is a significant process for generating DOM (Mayer et al., 2006, 2012; Pisani et al., 2011; Shank et al., 2011). Similarly, photo-dissolution may contribute to DBC generation from solid BC in aquatic environments (Alan Roebuck et al., 2017). In a natural aqueous environment, photo-dissolution from BC and photodegradation of DBC can take place simultaneously, making the photochemical process more complicated. By comparing the amount of DBC generated from BC with and without irradiation, Alan Roebuck et al. (2017) showed that photo-dissolution is a potential source of DBC in aquatic systems. However, the simultaneous or further photodegradation of newly generated DBC by photo-dissolution is poorly understood.

Overall, the potential mechanism for DBC photodegradation can be summarized as two pathways: (1) direct photodegradation and (2) radical-driven propagation reactions (Fig. 3). During the direct photodegradation process, the most photolabile fractions undergo primary photoreactions under sunlight irradiation of a prescribed wavelength and often generate the radicalized excited triplet states of DOM ($^3DOM^*$) (McNeill and Canonica, 2016), thus inducing the generation of singlet oxygen and superoxide (Fu et al., 2016; Zhou et al., 2018). These generated substances will further oxidize DOM through radical-driven reaction propagation. During this process, quenched radicals will be constantly regenerated and drive the transformation of DBC into lower molecular fractions, similar to the transformation of large fulvic and humic acid chromophores into smaller organic acids (Goldstone et al., 2002; Pullin et al., 2004).

1.3.2 Interaction between DBC and microorganisms

To date, few studies have investigated the interaction between DBC and microbes, which is in fact one of the most significant processes for DBC transformation and microbial community succession in aquatic environments. On the one hand, microbes can alter the molecular composition of DBC via catabolism and anabolism (Bostick et al., 2021; Chen et al., 2022; Goranov et al., 2022). On the other hand, DBC provides a unique habitat as a refractory carbon source and may thus affect the

constitution and succession of the microbial communities (Chen et al., 2022; Zhou et al., 2021).

BC has long been considered as a refractory fraction of the organic carbon pool and exhibits chemical stability and resistance to biodegradation. Its soluble fraction (DBC), however, is unlikely to be recalcitrant to microbial degradation. Qi et al. (2020) revealed the biodegradability of DBC via laboratory charcoal leaching experiments and a field study on DBC ^{14}C ages in rivers and oceans. They found that the DBC in rivers is predominantly young via ^{14}C ages, and no DBC accumulated in the microbe-active water during long-term leaching experiments. Norwood et al. (2013) subjected fresh DBC leached from charcoal to microbial incubation and found the removal of more than 50% of the total DBC within one month. Similarly, high biomineralization ratio (30%–70%) of biochar-derived DBC in 2–3 months were also reported in several studies (Bostick et al., 2021; Chen et al., 2022; Goranov et al., 2022). Such results provide direct evidence for the instability of DBC. However, the potential mechanisms driving the biomineralization of DBC are still unclear. One explanation is that DBC shows heterogeneous reactivity and the highly biolabile subcomponents in DBC may be easily degraded and even exhibit priming effects on bulk DBC biodegradation (Bianchi Thomas, 2011). Further study should underline the effects of biolabile fraction on DBC biodegradation possibly through subjecting DBC of varied aromaticity to microbial incubation.

Several studies have investigated the impact of DOM on the composition of microbial communities. Zhou et al. (2021) demonstrated that the source aromaticity of DOM influenced microbial community succession in aquatic environments. DOM with higher aromaticity exhibited much stronger environmental filtering of the microbial community. DBC is more aromatic than most DOM in nature and will inevitably change the microbial community structures in aquatic environments. Osterholz et al. (2016b) observed a strong correlation between DOM and total bacterial community composition in a pelagic marine system. In the DOM pool, some condensed aromatic components (representing DBC) partially correlated with DNA-based bacterial community composition, supporting the significant role of DBC in microbial activities. Some recent studies further provided direct evidence for microbial community variations related to DBC molecular structures (i.e., aliphatic compounds and condensed polycyclic aromatics) and incubation time (Chen et al., 2022; Zhang et al., 2020a). Moreover, Proteobacteria, which comprised a huge variety of nitrogen-fixing bacteria, proved to be the predominant phylum in DBC (Chen et al., 2022). Research hitherto has only concerned about the community succession in DBC. Thus,

further investigations regarding more aspects of DBC mineralization, such as the measurement of functional genes, should be conducted to better uncover the biogeochemical process of DBC.

In return, microbes also play a crucial role in regulating DBC transformation. Goranov et al. (2022) reported the microbial diversification of DBC molecules after 10 days of incubation, while Chen et al. (2022) demonstrated a decreased molecular diversity after 56 days of incubation. One possibility for this mismatch is the use of different feedstock types for DBC production and the choice of different photoirradiation intensity. Also, the different incubation time may also serve as an explanation. It is reasonable to speculate that the molecular composition of DBC may first become diversified and then less diverse. Further work should focus on the molecular shifts of DBC at different incubation time scales.

DBC is both photodegradable and biodegradable in nature. After photoirradiation, the aromaticity and bioavailability of DBC were constantly altered. The combined effects of photoirradiation and microbial utilization are of great significance as they are closely related to the cycling and turnover of DBC in an aquatic environment, where DBC is exposed to continuous photoirradiation and microbial utilization. Until recently, a few studies started to explore the effects of photodegradation on the biomineralization of DBC. An increased biomineralization ratio of DBC after photoirradiation was commonly observed (Bostick et al., 2021; Chen et al., 2022; Goranov et al., 2022). One probability is that the highly aromatic and recalcitrant subcomponents in DBC are decomposed into smaller sized aromatic clusters with higher bioavailability. Another explanation is that the photogenerated small molecules have priming effects on the further biodegradation of recalcitrant structures.

Hydrochar-derived DOM is also a type of DBC in a broad sense. Hao et al. (2018) compared the growth of cyanobacteria in DBC solutions extracted from a thermal series of bamboo hydrochar and determined that DBC samples with > 210 °C production temperatures exhibited a certain toxicity to cyanobacteria, with DBC produced at 300 °C causing the highest inhibition. However, 180 °C hydrochar-derived DBC and 500 °C biochar-derived DBC promoted the growth of cyanobacteria. Similarly, Zhang et al. (2021a) also revealed the general phytotoxicity of a thermal series of biochar-derived DBC on the germination of cabbage seeds. These results suggest that the production parameters of biochars and hydrochars should be optimized to guarantee safety toward aquatic systems by considering their toxicity toward aquatic organisms.

1.3.3 Interaction between DBC and pollutants

In recent decades, DOM has been proven to play a key role in the fate and transport of pollutants (Leal et al., 2013; Wenk et al., 2011; Zhou et al., 2017). Similarly, DBC can affect the transport and photodegradation of contaminants via sorption and photoproduction of reactive intermediates. Table 2 summarizes the available records for interactions between DBC and contaminants.

First, DBC exhibits a high adsorption capacity for hydrophobic pollutants. Their condensed aromatic structure has high hydrophobicity and can adsorb hydrophobic organic pollutants, especially hydrophobic organic contaminants, via hydrophobic interactions (Chin et al., 1997; Gauthier et al., 1987; Kopinke et al., 2001; Perminova et al., 1999). Besides, the pseudomicellar conformation of DBC could promote the binding interaction between DBC and hydrophobic organic contaminants (Fu et al., 2018a). Also, DBC contains abundant polar functional groups (e.g., carboxyl and hydroxyl groups) and can adsorb polar organic contaminants through hydrogen bonding and electrostatic interaction (Klaus et al., 1998; Senesi, 1992; Yamamoto et al., 2003). Furthermore, DBC can coordinate with heavy metals via complexation (Stubbins et al., 2010; Wu et al., 2011; Xia et al., 1997). Moreover, as DBC is defined as the water-soluble fraction of < 0.45 μm, it may exert some overlap with the definition of nano BC (< 1 μm) (Liu et al., 2018; Song et al., 2019) and holds pollutants well (Ramezanzadeh et al., 2021; Zhu et al., 2021). Tang et al. (2016) demonstrated that hydrophobic interactions were the main interaction mechanisms between DBC and polycyclic aromatic hydrocarbons (PAHs). Xu et al. (2020) revealed that coexisting Pb^{2+}, Cu^{2+}, Cd^{2+} and Zn^{2+} ions enhanced the aggregation and deposition of DBC via complexation and cation–π interactions, which helped to understand the fate of DBC and coexisting pollutants in environmental and engineering systems. Ramezanzadeh et al. (2021) found that nano BC was more effective at cadmium sorption in contaminated sandy soils than macro BC. Mahmoud et al. (2020) showed that nano BC was also a promising sorbent for phosphorus mainly through surface precipitation, potentially via complexation reactions between phosphorus and the mineral component in DBC.

Second, DBC can participate in the redox conversion processes of pollutants in the environment as a reactant or an electron transport carrier. Similar to NDOM, DBC contains a variety of redox-active organic molecules (e.g., those bearing quinoid, aromatic and thiol moieties). These species can act as reductants, reactive intermediaries or electron shuttles and affect the chemical and biological redox-mediated reactions of pollutants. Graber et al. (2014) demonstrated that DBC possessed significant redox activity and can promote the reduction and solubilization of Mn and Fe. In addition, DBC generated at lower production temperatures had a stronger redox ability. Dong et al. (2014) revealed that DBC could either act as an electron donor or an acceptor and efficiently reduce Cr(VI) or oxidize As(III), respectively.

Third, DBC can generate a large variety of reactive intermediates (e.g., $^3DBC^*$, ·OH, $^1O_2$, and O_2^-) under photoirradiation, which can promote not only its own photodegradation but also the photo-transformation of important pollutants (Fig. 3). It has been reported that the photo-reactivity of a DOM is closely associated with its aromaticity and molecular weight. DOM with higher aromaticity can absorb photons more efficiently (Boyle et al., 2009). Compared with NDOM, DBC has lower molecular weights and higher aromaticity (Qu et al., 2016; Zhou et al., 2018) and has proven to be one of the more photoactive components in the DOM pool. Thus, DBC may act as an efficient driver for the photo-transformation of contaminants. Fang et al. (2017) suggested that DBC contributed to the photodegradation of diethyl phthalate via the generation of ·OH and $^1O_2$. Serelis et al. (2021) compared the effects of biochar- and hydrochar-derived DBC on metribuzin photodegradation and observed that both char-derived DBC enhanced metribuzin photolysis, with hydrochar-derived DBC presenting a stronger optical filter effect and biochar-derived DBC exerting higher ability to generate ·OH and $^1O_2$. Zhou et al. (2018) found that DBC could significantly enhance the photo-transformation of 17β-estradiol by generating $^3DBC^*$ species. Tian et al. (2019) also proposed the same mechanism for chlortetracycline photo-transformation via $^3DBC^*$ attack. With respect to the photo-transformation of Ag^+ to nano Ag particles, the photo-reduction efficiency of DBC is higher than (Liu et al., 2021) or in opposition to those of NDOM (Wan et al., 2021). Furthermore, Wang et al. (2020) investigated the effects of DBC on the photodegradation of 24 pharmaceutically active compounds and demonstrated that DBC could accelerate the photodegradation of such contaminants that were susceptible to one-electron oxidation by $^3DBC^*$. Moreover, both the laboratory prepared and naturally occurring DBC are expected to contain mineral compositions, which could serve as a natural photocatalyst mediating the photo-redox reactions of pollutants (Fu et al., 2018b).

In addition, DBC can also affect the environmental behaviors of some emerging contaminants. For example, DBC can be strongly adsorbed on the surfaces of nano-Ag, facilitating DBC transport in porous media (Wang et al., 2021). In addition, DBC can enhance the destabilization and deposition of polystyrene by reducing

Table 2 Effects of DBC on the fate and transport of pollutants

Biomass	Temperature (°C)	Pollutants	Interaction mechanism	Results	References
Sewage sludge, soybean strown, rice straw, peanut and mushroom residue biochar	500	PAHs	Sorption	DBC of higher humification degrees possessed higher sorption capacities for PAHs	(Tang et al., 2016)
Peanut shell	200, 400, 500	Phenanthrene	Sorption	Capacity: 200 °C DBC > 400 °C DBC > 500 °C DBC	(Ma et al., 2020)
Wood	400, 600	Zwitterionic ciprofloxacin	Sorption and co-transport	Aging and sorption resulted in destabilization of DBC, and further impeded the co-transport of zwitterionic ciprofloxacin	(Zhu et al., 2021)
Rice straw	450	Pb	Sorption	More binding sites for Pb on DBC than NDOM	(Huang et al., 2020)
Wood	650	Cd^{2+}	Sorption	Nanobiochar was more effective at Cd^{2+} sorption than macrobiochar	(Ramezanzadeh et al., 2021)
Rice husk	400	As(III)	Complexation	Enhanced the non-oxidative and oxidative precipitation of As(III) via complexation	(Zhong et al., 2020)
Maize straw	500	Pb^{2+}, Cu^{2+}, Cd^{2+}, Zn^{2+}	Complexation and cation–π interaction	Coexisting heavy metals enhanced the aggregation and deposition of DBC ($Pb^{2+} > Cu^{2+} > Cd^{2+} > Zn^{2+}$)	(Xu et al., 2020)
Eucalyptus wood, olive pomace and greenhouse waste	350, 450, 600, 800	Mn and Fe	Reduction and solubilization	DBC produced at lower temperatures had higher reducing capacities and they can solubilized Fe and Mn to a higher degree	(Graber et al., 2014)
Sugar beet tailing and Brazilian pepper	300	Cr(VI) and As(III)	Redox reaction	DBC can serve as electron donors or acceptors, and enhance Cr(VI) reduction or As(III) oxidation, respectively; Cr(VI) and As(III) comprised a redox couple	(Dong et al., 2014)
Rice straw	400	$Ag^{+} \rightarrow nAg$	1) Sorption (LMCT) 2) Photoreduction (O_2^{-})	The efficiency of photo-reduction of Ag^{+} by DBC was higher than by NDOM	(Liu et al., 2021)
Soybean, peanut, rice	400	$Hg(II) \rightarrow Hg(0)$	Photoreduction (O_2^{-})	Led to a unique positive mass-independent isotopic fractionation of Hg(0), in contrast with the effect of NDOM	(Li et al., 2020)
Rice, corn, and wheat straw	400	PPCPs	Photodegradation ($^3DBC^*$, $^1O_2$, and $\cdot OH$)	Efficiency: rice > corn > wheat; Main mechanism: $^3DBC^* > \cdot OH > > ^1O_2$	(Wan et al., 2021)
Maize straw and pig manure	300, 500	Imidacloprid	Photodegradation	$^1O_2$ played a predominant role in the photodegradation of imidacloprid	(Zhang et al., 2020b)
Bamboo	400	17β-estradiol	Photo-transformation ($^3DBC^*$)	DBC exhibited higher mediation efficiency for facilitating the photo-transformation of 17β-estradiol than dissolved humic substances by generating more $^3DBC^*$ species	(Zhou et al., 2018)

Table 2 (continued)

Biomass	Temperature (°C)	Pollutants	Interaction mechanism	Results	References
Bamboo	400	Chlortetracycline	Photo-transformation ($^3DBC^*$)	DBC significantly enhanced the photo-transformation of chlortetracycline by generating $^3DBC^*$ species to attack the amidogen in chlortetracycline; The photosensitization of DBC was closely related to its carbonyl components	(Tian et al., 2019)
Pine needles and wheat straws	300, 500	Diethyl phthalate	Photodegradation (•OH and $^1O_2$)	DBC produced at higher temperatures were more efficient in degrading diethyl phthalate; Potential mechanism: •OH and $^1O_2$	(Fang et al., 2017)
Maize	300, 500	Nano-Ag	Sorption	Facilitated the transport of nano-Ag through surface adsorption	(Wang et al., 2021)
Wood, maize, and rice straw	300, 500	PS	Sorption	Enhanced the aggregation and deposition of PS, in contrast with the effect of NDOM; Such effects were weaker for aged PS	(Xu et al., 2021)

Chen *et al. Carbon Research*   (2022) 1:23

Page 15 of 19

electrostatic repulsion, which is in contrast to the effect of humic acid (Xu et al., 2021).

As one of the most labile and mobile fractions in the BC continuum (Wang et al., 2013), DBC can easily be released via soil infiltration and surface runoff (Dittmar et al., 2012a; Jaffe et al., 2013). The potential role of mobile DBC as a carrier of contaminants may query the role of BC as long-term remediation materials. Thus, more efforts should be made to uncover the interaction mechanisms between DBC and pollutants to better evaluate the applicability of BC in immobilizing pollutants.

2 Future perspectives

To better understand the environmental behavior of DBC, further efforts should be made to develop new technologies of higher precision and resolution, as well as jointly apply existing advanced techniques, such as combined utilization of FT-ICR-MS and BPCA, GC–MS and ^{13}C-NMR. Available studies have mainly focused on the photodegradation processes of DBC. Information regarding the microbial transformations of DBC molecules, the impact of DBC on microflora and expression of C metabolism- and N-related functional genes, and the transformation and degradation of coexisting pollutants regulated by DBC, however, is far from robust. In addition, the lack of direct comparisons between the environmental transformation processes for DBC and NDOM, such as the different degradability, the preferential degradation or utilization of different molecular during photodegradation and biodegradation, and the different role of ROS plays in regulating their photo-transformation, increase the complexity of distinguishing the environmental behaviors of DBC. Photodegradation and biodegradation processes occur simultaneously in real environments. As such, both processes should be considered in evaluating the stability of DBC. After photoirradiation, the aromaticity, molecular weights and methyl functional groups of DBC decrease. Therefore, it is plausible to hypothesize that the residual DBC may be more bioavailable. Only a few studies started to focus on the biodegradation of photobleached DBC; however, the simultaneous photodegradation and biodegradation of DBC still merits further investigation. In recent years, the selective protection of different components in DOM by minerals has been widely reported. Similarly, after selectively adsorbed to minerals, the subsequent biodegradation of the presumably protected DBC fractions is largely unknown and may contribute to the understanding of the fate of DBC in real environment.

Abbreviations
DBC: Dissolved black carbon; BC: Black carbon; DOM: Dissolved organic matter; NDOM: Natural dissolved organic matter; CTO: Chemothermal oxidation; BPCA: Benzene polycarboxylic acid; CSRA: Compound-specific radiocarbon analysis; FT-ICR-MS: Fourier transform ion cyclotron resonance mass spectrometry; AI$_{mod}$: Modified aromaticity index; NOSC: Nominal oxygen state of carbon; SPE: Solid-phase extraction; ESI: Electrospray ionization; EEM: Three-dimensional fluorescence; DBE: Double bond equivalent; ConAC: Condensed aromatic carbon; PAHs: Polycyclic aromatic hydrocarbons.

Author's contributions
Yalan Chen, Ke Sun and Baoshan Xing contributed to the study conception and design. Material preparation, data collection and analysis were performed by Yalan Chen, Zhibo Wang, Enyao Zhang and Yan Yang. The first draft of the manuscript was written by Yalan Chen. Ke Sun and Baoshan Xing assisted in the review and editing of the manuscript. All authors read and approved the final manuscript.

Availability of data and materials
The datasets used or analyzed during the current study are available from the corresponding author on reasonable request.

Declarations

Competing interests
Ke Sun and Baoshan Xing are editorial board members of Carbon Research and were not involved in the editorial review, or the decision to publish, this article. All authors declare that there are no competing interests.

Author details
[1]State Key Laboratory of Water Environment Simulation, School of Environment, Beijing Normal University, Beijing 100875, China. [2]Stockbridge School of Agriculture, University of Massachusetts, Amherst, MA 01003, USA.

References
Abdul Jameel AG, Khateeb A, Elbaz AM, Emwas A-H, Zhang W, Roberts WL, Sarathy SM (2019) Characterization of deasphalted heavy fuel oil using APPI (+) FT-ICR mass spectrometry and NMR spectroscopy. Fuel 253:950–963. https://doi.org/10.1016/j.fuel.2019.05.061

Alan Roebuck J, Podgorski DC, Wagner S, Jaffé R (2017) Photodissolution of charcoal and fire-impacted soil as a potential source of dissolved black carbon in aquatic environments. Org Geochem 112:16–21. https://doi.org/10.1016/j.orggeochem.2017.06.018

Bianchi Thomas S (2011) The role of terrestrially derived organic carbon in the coastal ocean: a changing paradigm and the priming effect. Proc Natl Acad Sci 108:19473–19481. https://doi.org/10.1073/pnas.1017982108

Bittar TB, Vieira AAH, Stubbins A, Mopper K (2015) Competition between photochemical and biological degradation of dissolved organic matter from the cyanobacteria Microcystis aeruginosa. Limnol Oceanogr 60:1172–1194. https://doi.org/10.1002/lno.10090

Bostick K W, Zimmerman A R, Wozniak A S, Mitra S, Hatcher P G (2018) Production and Composition of Pyrogenic Dissolved Organic Matter From a Logical Series of Laboratory-Generated Chars. 6. https://doi.org/10.3389/feart.2018.00043

Bostick K W, Zimmerman A R, Goranov A I, Mitra S, Hatcher P G, Wozniak A S (2021) Biolability of Fresh and Photodegraded Pyrogenic Dissolved Organic Matter From Laboratory-Prepared Chars. *Journal of Geophysical Research: Biogeosciences* 126: e2020JG005981. https://doi.org/10.1029/2020JG005981

Chen *et al. Carbon Research*   (2022) 1:23

Page 16 of 19

Bostick KW, Zimmerman AR, Goranov AI, Mitra S, Hatcher PG, Wozniak AS (2020) Photolability of pyrogenic dissolved organic matter from a thermal series of laboratory-prepared chars. Sci Total Environ 724:138198. https://doi.org/10.1016/j.scitotenv.2020.138198

Boyle ES, Guerriero N, Thiallet A, Vecchio RD, Blough NV (2009) Optical Properties of Humic Substances and CDOM: Relation to Structure. Environ Sci Technol 43:2262–2268. https://doi.org/10.1021/es803264g

Bruun S, Jensen ES, Jensen LS (2008) Microbial mineralization and assimilation of black carbon: Dependency on degree of thermal alteration. Org Geochem 39:839–845. https://doi.org/10.1016/j.orggeochem.2008.04.020

Cao X, Aiken GR, Spencer RGM, Butler K, Mao J, Schmidt-Rohr K (2016) Novel insights from NMR spectroscopy into seasonal changes in the composition of dissolved organic matter exported to the Bering Sea by the Yukon River. Geochim Cosmochim Acta 181:72–88. https://doi.org/10.1016/j.gca.2016.02.029

Chen J, Gu B, LeBoeuf EJ, Pan H, Dai S (2002) Spectroscopic characterization of the structural and functional properties of natural organic matter fractions. Chemosphere 48:59–68. https://doi.org/10.1016/S0045-6535(02)00041-3

Chen W, Westerhoff P, Leenheer JA, Booksh K (2003) Fluorescence excitation—emission matrix regional integration to quantify spectra for dissolved organic matter. Environ Sci Technol 37:5701–5710. https://doi.org/10.1021/es034354c

Chen M, Kim S, Park J-E, Jung H-J, Hur J (2016) Structural and compositional changes of dissolved organic matter upon solid-phase extraction tracked by multiple analytical tools. Anal Bioanal Chem 408:6249–6258. https://doi.org/10.1007/s00216-016-9728-0

Chen Y, Sun K, Sun H, Yang Y, Han L, Zheng H, Xing B (2020) Investigation on parameters optimization to produce hydrochar without carbohydrate carbon. Sci Total Environ 748:141354. https://doi.org/10.1016/j.scitotenv.2020.141354

Chen Y, Sun K, Sun H, Yang Y, Li Y, Gao B, Xing B (2022) Photodegradation of pyrogenic dissolved organic matter increases bioavailability: Novel insight into bioalteration, microbial community succession, and C and N dynamics. Chem Geol 605:120964. https://doi.org/10.1016/j.chemgeo.2022.120964

Chin Y-P, Aiken GR, Danielsen KM (1997) Binding of pyrene to aquatic and commercial humic substances: the role of molecular weight and aromaticity. Environ Sci Technol 31:1630–1635. https://doi.org/10.1021/es960404k

Coppola AI, Druffel ERM (2016) Cycling of black carbon in the ocean. Geophys Res Lett 43:4477–4482. https://doi.org/10.1002/2016GL068574

Coppola AI, Wiedemeier DB, Galy V, Haghipour N, Hanke UM, Nascimento GS, Usman M, Blattmann TM, Reisser M, Freymond CV, Zhao M, Voss B, Wacker L, Schefuß E, Peucker-Ehrenbrink B, Abiven S, Schmidt MWI, Eglinton TI (2018) Global-scale evidence for the refractory nature of riverine black carbon. Nat Geosci 11:584–588. https://doi.org/10.1038/s41561-018-0159-8

Coppola AI, Seidel M, Ward ND, Viviroli D, Nascimento GS, Haghipour N, Revels BN, Abiven S, Jones MW, Richey JE, Eglinton TI, Dittmar T, Schmidt MWI (2019) Marked isotopic variability within and between the Amazon River and marine dissolved black carbon pools. Nat Commun 10:4018. https://doi.org/10.1038/s41467-019-11543-9

Ding Y, Yamashita Y, Dodds WK, Jaffé R (2013) Dissolved black carbon in grassland streams: Is there an effect of recent fire history? Chemosphere 90:2557–2562. https://doi.org/10.1016/j.chemosphere.2012.10.098

Dittmar T (2008) The molecular level determination of black carbon in marine dissolved organic matter. Org Geochem 39:396–407. https://doi.org/10.1016/j.orggeochem.2008.01.015

Dittmar T, Koch BP (2006) Thermogenic organic matter dissolved in the abyssal ocean. Mar Chem 102:208–217. https://doi.org/10.1016/j.marchem.2006.04.003

Dittmar T, Paeng J (2009) A heat-induced molecular signature in marine dissolved organic matter. Nat Geosci 2:175–179. https://doi.org/10.1038/ngeo440

Dittmar T, de Rezende CE, Manecki M, Niggemann J, Coelho Ovalle AR, Stubbins A, Bernardes MC (2012a) Continuous flux of dissolved black carbon from a vanished tropical forest biome. Nat Geosci 5:618–622. https://doi.org/10.1038/ngeo1541

Dittmar T, Paeng J, Gihring TM, Suryaputra IGNA, Huettel M (2012b) Discharge of dissolved black carbon from a fire-affected intertidal system. Limnol Oceanogr 57:1171–1181. https://doi.org/10.4319/lo.2012.57.4.1171

Dong X, Ma LQ, Gress J, Harris W, Li Y (2014) Enhanced Cr(VI) reduction and As(III) oxidation in ice phase: Important role of dissolved organic matter from biochar. J Hazard Mater 267:62–70. https://doi.org/10.1016/j.jhazmat.2013.12.027

Enke CG (1997) A predictive model for matrix and analyte effects in electrospray ionization of singly-charged ionic analytes. Anal Chem 69:4885–4893. https://doi.org/10.1021/ac970095w

Fang G, Liu C, Wang Y, Dionysiou DD, Zhou D (2017) Photogeneration of reactive oxygen species from biochar suspension for diethyl phthalate degradation. Appl Catal B 214:34–45. https://doi.org/10.1016/j.apcatb.2017.05.036

Fu H, Liu H, Mao J, Chu W, Li Q, Alvarez PJJ, Qu X, Zhu D (2016) Photochemistry of dissolved black carbon released from biochar: reactive oxygen species generation and phototransformation. Environ Sci Technol 50:1218–1226. https://doi.org/10.1021/acs.est.5b04314

Fu H, Wei C, Qu X, Li H, Zhu D (2018) Strong binding of apolar hydrophobic organic contaminants by dissolved black carbon released from biochar: a mechanism of pseudomicelle partition and environmental implications. Environ Pollut 232:402–410. https://doi.org/10.1016/j.envpol.2017.09.053

Fu H, Zhou Z, Zheng S, Xu Z, Alvarez PJJ, Yin D, Qu X, Zhu D (2018) Dissolved mineral ash generated by vegetation fire is photoactive under the solar spectrum. Environ Sci Technol 52:10453–10461. https://doi.org/10.1021/acs.est.8b03010

Gauthier TD, Seitz WR, Grant CL (1987) Effects of structural and compositional variations of dissolved humic materials on pyrene Koc values. Environ Sci Technol 21:243–248. https://doi.org/10.1021/es00157a003

Glaser B, Haumaier L, Guggenberger G, Zech W (1998) Black carbon in soils: the use of benzenecarboxylic acids as specific markers. Org Geochem 29:811–819. https://doi.org/10.1016/S0146-6380(98)00194-6

Goldstone JV, Pullin MJ, Bertilsson S, Voelker BM (2002) Reactions of hydroxyl radical with humic substances: bleaching, mineralization, and production of bioavailable carbon substrates. Environ Sci Technol 36:364–372. https://doi.org/10.1021/es0109646

Goranov AI, Wozniak AS, Bostick KW, Zimmerman AR, Mitra S, Hatcher PG (2020) Photochemistry after fire: Structural transformations of pyrogenic dissolved organic matter elucidated by advanced analytical techniques. Geochim Cosmochim Acta 290:271–292. https://doi.org/10.1016/j.gca.2020.08.030

Goranov AI, Wozniak AS, Bostick KW, Zimmerman AR, Mitra S, Hatcher PG (2022) Microbial labilization and diversification of pyrogenic dissolved organic matter. Biogeosciences 19:1491–1514. https://doi.org/10.5194/bg-19-1491-2022

Graber ER, Tsechansky L, Lew B, Cohen E (2014) Reducing capacity of water extracts of biochars and their solubilization of soil Mn and Fe. Eur J Soil Sci 65:162–172. https://doi.org/10.1111/ejss.12071

Gustafsson Ö, Bucheli TD, Kukulska Z, Andersson M, Largeau C, Rouzaud J-N, Reddy CM, Eglinton TI (2001) Evaluation of a protocol for the quantification of black carbon in sediments. Global Biogeochem Cycles 15:881–890. https://doi.org/10.1029/2000GB001380

Han L, Nie X, Wei J, Gu M, Wu W, Chen M (2021) Effects of feedstock biopolymer compositions on the physiochemical characteristics of dissolved black carbon from lignocellulose-based biochar. Sci Total Environ 751:141491. https://doi.org/10.1016/j.scitotenv.2020.141491

Hao S, Zhu X, Liu Y, Qian F, Fang Z, Shi Q, Zhang S, Chen J, Ren ZJ (2018) Production temperature effects on the structure of hydrochar-derived dissolved organic matter and associated toxicity. Environ Sci Technol 52:7486–7495. https://doi.org/10.1021/acs.est.7b04983

Helms JR, Stubbins A, Ritchie JD, Minor EC, Kieber DJ, Mopper K (2008) Absorption spectral slopes and slope ratios as indicators of molecular weight, source, and photobleaching of chromophoric dissolved organic matter. Limnol Oceanogr 53:955–969. https://doi.org/10.4319/lo.2008.53.3.0955

Helms JR, Mao J, Chen H, Perdue EM, Green NW, Hatcher PG, Mopper K, Stubbins A (2015) Spectroscopic characterization of oceanic dissolved organic matter isolated by reverse osmosis coupled with electrodialysis. Mar Chem 177:278–287. https://doi.org/10.1016/j.marchem.2015.07.007

Hertkorn N, Harir M, Cawley KM, Schmitt-Kopplin P, Jaffé R (2016) Molecular characterization of dissolved organic matter from subtropical wetlands: a comparative study through the analysis of optical properties, NMR and FTICR/MS. Biogeosciences 13:2257–2277. https://doi.org/10.5194/bg-13-2257-2016

Chen *et al. Carbon Research*   (2022) 1:23

Page 17 of 19

Herzsprung P, v. Tümpling W, Hertkorn N, Harir M, Friese K, Schmitt-Kopplin P, (2015) High-field FTICR-MS data evaluation of natural organic matter: are CHON5S2 molecular class formulas assigned to 13C isotopic m/z and in reality CHO components? Anal Chem 87:9563–9566. https://doi.org/10.1021/acs.analchem.5b02549

Herzsprung P, Hertkorn N, von Tümpling W, Harir M, Friese K, Schmitt-Kopplin P (2014) Understanding molecular formula assignment of Fourier transform ion cyclotron resonance mass spectrometry data of natural organic matter from a chemical point of view. Anal Bioanal Chem 406:7977–7987. https://doi.org/10.1007/s00216-014-8249-y

Hockaday WC, Grannas AM, Kim S, Hatcher PG (2006) Direct molecular evidence for the degradation and mobility of black carbon in soils from ultrahigh-resolution mass spectral analysis of dissolved organic matter from a fire-impacted forest soil. Org Geochem 37:501–510. https://doi.org/10.1016/j.orggeochem.2005.11.003

Hockaday WC, Grannas AM, Kim S, Hatcher PG (2007) The transformation and mobility of charcoal in a fire-impacted watershed. Geochim Cosmochim Acta 71:3432–3445. https://doi.org/10.1016/j.gca.2007.02.023

Huang M, Li Z, Chen M, Wen J, Luo N, Xu W, Ding X, Xing W (2020) Dissolved organic matter released from rice straw and straw biochar: Contrasting molecular composition and lead binding behaviors. Sci Total Environ 739:140378. https://doi.org/10.1016/j.scitotenv.2020.140378

Huang M, Li Z, Wen J, Ding X, Zhou M, Cai C, Shen F (2021) Molecular insights into the effects of pyrolysis temperature on composition and copper binding properties of biochar-derived dissolved organic matter. J Hazard Mater 410:124537. https://doi.org/10.1016/j.jhazmat.2020.124537

Jaffé R, Yamashita Y, Maie N, Cooper WT, Dittmar T, Dodds WK, Jones JB, Myoshi T, Ortiz-Zayas JR, Podgorski DC, Watanabe A (2012) Dissolved organic matter in headwater streams: compositional variability across climatic regions of North America. Geochim Cosmochim Acta 94:95–108. https://doi.org/10.1016/j.gca.2012.06.031

Jaffe R, Ding Y, Niggemann J, Vahatalo AV, Stubbins A, Spencer RGM, Campbell J, Dittmar T (2013) Global charcoal mobilization from soils via dissolution and riverine transport to the oceans. Science 340:345–347. https://doi.org/10.1126/science.1231476

Jones MW, Santín C, van der Werf GR, Doerr SH (2019) Global fire emissions buffered by the production of pyrogenic carbon. Nat Geosci 12:742–747. https://doi.org/10.1038/s41561-019-0403-x

K Hammes MWI Schmidt RJ Smernik LA Currie WP Ball TH Nguyen P Louchouarn S Houel Ö Gustafsson M Elmquist G Cornelissen JO Skjemstad CA Masiello J Song P Peng a, Mitra S, Dunn J C, Hatcher P G, Hockaday W C, Smith D M, Hartkopf-Fröder C, Böhmer A, Lüer B, Huebert B J, Amelung W, Brodowski S, Huang L, Zhang W, Gschwend P M, Flores-Cervantes D X, Largeau C, Rouzaud J-N, Rumpel C, Guggenberger G, Kaiser K, Rodionov A, Gonzalez-Vila F J, Gonzalez-Perez J A, de la Rosa J M, Manning D A C, López-Capél E, Ding L, 2007 Comparison of quantification methods to measure fire-derived (black/elemental) carbon in soils and sediments using reference materials from soil, water, sediment and the atmosphere Global Biogeochem Cycles 21 https://doi.org/10.1029/2006GB002914

Kim S, Kaplan LA, Benner R, Hatcher PG (2004) Hydrogen-deficient molecules in natural riverine water samples—evidence for the existence of black carbon in DOM. Mar Chem 92:225–234. https://doi.org/10.1016/j.marchem.2004.06.042

Klaus U, Mohamed S, Volk M, Spiteller M (1998) Interaction of aquatic substances with anilazine and its derivatives: The nature of the bound residues. Chemosphere 37:341–361. https://doi.org/10.1016/S0045-6535(98)00050-2

Koch BP, Dittmar T (2006) From mass to structure: an aromaticity index for high-resolution mass data of natural organic matter. Rapid Commun Mass Spectrom 20:926–932. https://doi.org/10.1002/rcm.2386

Koch BP, Dittmar T, Witt M, Kattner G (2007) Fundamentals of molecular formula assignment to ultrahigh resolution mass data of natural organic matter. Anal Chem 79:1758–1763. https://doi.org/10.1021/ac061949s

Kopinke F-D, Georgi A, Mackenzie K (2001) Sorption of pyrene to dissolved humic substances and related model polymers. 1. structure—property correlation. Environ Sci Technol 35:2536–2542. https://doi.org/10.1021/es000233q

Kujawinski EB, Behn MD (2006) Automated analysis of electrospray ionization fourier transform ion cyclotron resonance mass spectra of natural organic matter. Anal Chem 78:4363–4373. https://doi.org/10.1021/ac0600306

Kujawinski EB, Del Vecchio R, Blough NV, Klein GC, Marshall AG (2004) Probing molecular-level transformations of dissolved organic matter: insights on photochemical degradation and protozoan modification of DOM from electrospray ionization Fourier transform ion cyclotron resonance mass spectrometry. Mar Chem 92:23–37. https://doi.org/10.1016/j.marchem.2004.06.038

LA Ziolkowski ERM Druffel 2010 Aged black carbon identified in marine dissolved organic carbon Geophys Res Lett 37 https://doi.org/10.1029/2010GL043963

Latch DE, Stender BL, Packer JL, Arnold WA, McNeill K (2003) Photochemical fate of pharmaceuticals in the environment: cimetidine and ranitidine. Environ Sci Technol 37:3342–3350. https://doi.org/10.1021/es0340782

Leal JF, Esteves VI, Santos EBH (2013) BDE-209: kinetic studies and effect of humic substances on photodegradation in water. Environ Sci Technol 47:14010–14017. https://doi.org/10.1021/es4035254

Li Z-K, Wei X-Y, Yan H-L, Zong Z-M (2015) Insight into the structural features of Zhaotong lignite using multiple techniques. Fuel 153:176–182. https://doi.org/10.1016/j.fuel.2015.02.117

Li Y, Harir M, Uhl J, Kanawati B, Lucio M, Smirnov KS, Koch BP, Schmitt-Kopplin P, Hertkorn N (2017) How representative are dissolved organic matter (DOM) extracts? a comprehensive study of sorbent selectivity for DOM isolation. Water Res 116:316–323. https://doi.org/10.1016/j.watres.2017.03.038

Li L, Wang X, Fu H, Qu X, Chen J, Tao S, Zhu D (2020) Dissolved black carbon facilitates photoreduction of Hg(II) to Hg(0) and reduces mercury uptake by lettuce (Lactuca sativa L.). Environ Sci Technol 54:11137–11145. https://doi.org/10.1021/acs.est.0c01132

Lin P, Rincon AG, Kalberer M, Yu JZ (2012) Elemental composition of HULIS in the pearl river delta region, China: results Inferred from positive and negative electrospray high resolution mass spectrometric data. Environ Sci Technol 46:7454–7462. https://doi.org/10.1021/es300285d

Liu F-J, Wei X-Y, Wang Y-G, Li P, Li Z-K, Zong Z-M (2015) Sulfur-containing species in the extraction residue from Xianfeng lignite characterized by X-ray photoelectron spectrometry and electrospray ionization Fourier transform ion cyclotron resonance mass spectrometry. RSC Adv 5:7125–7130. https://doi.org/10.1039/c4ra12435a

Liu G, Zheng H, Jiang Z, Zhao J, Wang Z, Pan B, Xing B (2018) Formation and physicochemical characteristics of nano biochar: insight into chemical and colloidal stability. Environ Sci Technol 52:10369–10379. https://doi.org/10.1021/acs.est.8b01481

Liu H, Ge Q, Xu F, Qu X, Fu H, Sun J (2021) Dissolved black carbon induces fast photo-reduction of silver ions under simulated sunlight. Sci Total Environ 775:145897. https://doi.org/10.1016/j.scitotenv.2021.145897

Liu Y, Wang M, Yin S, Xie L, Qu X, Fu H, Shi Q, Zhou F, Xu F, Tao S, Zhu D (2022) Comparing photoactivities of dissolved organic matter released from rice straw-pyrolyzed biochar and composted rice straw. Environ Sci Technol 56:2803–2815. https://doi.org/10.1021/acs.est.1c08061

Ma Y, Chen Q, Chen Y, Wang L, Wu M (2020) Environmental behavior of dissolved black carbon from peanut shell biochar on phenanthrene. Environ Pollut Cont 42:985–989

Mahmoud E, El Baroudy A, Ali N, Sleem M (2020) Spectroscopic studies on the phosphorus adsorption in salt-affected soils with or without nano-biochar additions. Environ Res 184:109277. https://doi.org/10.1016/j.envres.2020.109277

Mannino A, Rodger Harvey H (2004) Black carbon in estuarine and coastal ocean dissolved organic matter. Limnol Oceanogr 49:735–740. https://doi.org/10.4319/lo.2004.49.3.0735

Marshall AG, Hendrickson CL, Jackson GS (1998) Fourier transform ion cyclotron resonance mass spectrometry: a primer. Mass Spectrom Rev 17:1–35.

Masiello CA, Druffel ERM (1998) Black Carbon in Deep-Sea Sediments. Science 280:1911. https://doi.org/10.1126/science.280.5371.1911

Mayer LM, Schick LL, Skorko K, Boss E (2006) Photodissolution of particulate organic matter from sediments. Limnol Oceanogr 51:1064–1071. https://doi.org/10.4319/lo.2006.51.2.1064

Mayer LM, Thornton KR, Schick LL, Jastrow JD, Harden JW (2012) Photodissolution of soil organic matter. Geoderma 170:314–321. https://doi.org/10.1016/j.geoderma.2011.11.030

McNeill K, Canonica S (2016) Triplet state dissolved organic matter in aquatic photochemistry: reaction mechanisms, substrate scope, and photophysical properties. Environmental Science-Processes & Impacts 18:1381–1399. https://doi.org/10.1039/c6em00408c

Chen *et al. Carbon Research*   (2022) 1:23

Page 18 of 19

Mori Y, Nishioka J, Fujio S, Yamashita Y (2021) Transport of dissolved black carbon from marginal sea sediments to the western North Pacific. Prog Oceanogr 193:102552. https://doi.org/10.1016/j.pocean.2021.102552

Murphy KR, Stedmon CA, Wenig P, Bro R (2014) OpenFluor– an online spectral library of auto-fluorescence by organic compounds in the environment. Anal Methods 6:658–661. https://doi.org/10.1039/C3AY41935E

Nguyen TH, Brown RA, Ball WP (2004) An evaluation of thermal resistance as a measure of black carbon content in diesel soot, wood char, and sediment. Org Geochem 35:217–234. https://doi.org/10.1016/j.orggeochem.2003.09.005

Norwood MJ, Louchouarn P, Kuo L-J, Harvey OR (2013) Characterization and biodegradation of water-soluble biomarkers and organic carbon extracted from low temperature chars. Org Geochem 56:111–119. https://doi.org/10.1016/j.orggeochem.2012.12.008

Reisser M, Purves R S, Schmidt M W I, Abiven S (2016) Pyrogenic Carbon in Soils: A Literature-Based Inventory and a Global Estimation of Its Content in Soil Organic Carbon and Stocks. 4. https://doi.org/10.3389/feart.2016.00080

RGM Spencer A Stubbins PJ Hernes A Baker K Mopper AK Aufdenkampe RY Dyda VL Mwamba AM Mangangu JN Wabakanghanzi J Six 2009 Photochemical degradation of dissolved organic matter and dissolved lignin phenols from the Congo River J Geophys Res Biogeosci 114 https://doi.org/10.1029/2009JG000968

Ohno T, Sleighter RL, Hatcher PG (2016) Comparative study of organic matter chemical characterization using negative and positive mode electrospray ionization ultrahigh-resolution mass spectrometry. Anal Bioanal Chem 408:2497–2504. https://doi.org/10.1007/s00216-016-9346-x

Osterholz H, Kirchman D L, Niggemann J, Dittmar T (2016a) Environmental Drivers of Dissolved Organic Matter Molecular Composition in the Delaware Estuary. 4. https://doi.org/10.3389/feart.2016a.00095

Osterholz H, Singer G, Wemheuer B, Daniel R, Simon M, Niggemann J, Dittmar T (2016b) Deciphering associations between dissolved organic molecules and bacterial communities in a pelagic marine system. ISME J 10:1717–1730. https://doi.org/10.1038/ismej.2015.231

Perminova IV, Grechishcheva NY, Petrosyan VS (1999) Relationships between structure and binding affinity of humic substances for polycyclic aromatic hydrocarbons: relevance of molecular descriptors. Environ Sci Technol 33:3781–3787. https://doi.org/10.1021/es990056x

Pisani O, Yamashita Y, Jaffé R (2011) Photo-dissolution of flocculent, detrital material in aquatic environments: Contributions to the dissolved organic matter pool. Water Res 45:3836–3844. https://doi.org/10.1016/j.watres.2011.04.035

Porto CFC, Pinto FE, Souza LM, Madeira NCL, Neto ÁC, de Menezes SMC, Chinelatto LS, Freitas CS, Vaz BG, Lacerda V, Romão W (2019) Characterization of organosulfur compounds in asphalt cement samples by ESI(+)FT-ICR MS and 13C NMR spectroscopy. Fuel 256:115923. https://doi.org/10.1016/j.fuel.2019.115923

Preston CM, Schmidt MWI (2006) Black (pyrogenic) carbon: a synthesis of current knowledge and uncertainties with special consideration of boreal regions. Biogeosciences 3:397–420. https://doi.org/10.5194/bg-3-397-2006

Pullin MJ, Bertilsson S, Goldstone JV, Voelker BM (2004) Effects of sunlight and hydroxyl radical on dissolved organic matter: Bacterial growth efficiency and production of carboxylic acids and other substrates. Limnol Oceanogr 49:2011–2022. https://doi.org/10.4319/lo.2004.49.6.2011

Qi Y, Fu W, Tian J, Luo C, Shan S, Sun S, Ren P, Zhang H, Liu J, Zhang X, Wang X (2020) Dissolved black carbon is not likely a significant refractory organic carbon pool in rivers and oceans. Nat Commun 11:5051. https://doi.org/10.1038/s41467-020-18808-8

Qu X, Fu H, Mao J, Ran Y, Zhang D, Zhu D (2016) Chemical and structural properties of dissolved black carbon released from biochars. Carbon 96:759–767. https://doi.org/10.1016/j.carbon.2015.09.106

Ramezanzadeh H, Reyhanitabar A, Oustan S, Mohammadi MH, Zee SEATM, v d, (2021) Enhanced sorption of cadmium by using biochar nanoparticles from ball milling in a sandy soil. Eurasian Soil Sci 54:201–211. https://doi.org/10.1134/S1064229321020125

Riedel T, Biester H, Dittmar T (2012) Molecular fractionation of dissolved organic matter with metal salts. Environ Sci Technol 46:4419–4426. https://doi.org/10.1021/es203901u

Schmidt A, Karas M, Dülcks T (2003) Effect of different solution flow rates on analyte ion signals in nano-ESI MS, or: when does ESI turn into nano-ESI? J Am Soc Mass Spectrom 14:492–500. https://doi.org/10.1016/S1044-0305(03)00128-4

Schneider MPW, Hilf M, Vogt UF, Schmidt MWI (2010) The benzene polycarboxylic acid (BPCA) pattern of wood pyrolyzed between 200℃ and 1000℃. Org Geochem 41:1082–1088. https://doi.org/10.1016/j.orggeochem.2010.07.001

Seidel M, Beck M, Riedel T, Waska H, Suryaputra IGNA, Schnetger B, Niggemann J, Simon M, Dittmar T (2014) Biogeochemistry of dissolved organic matter in an anoxic intertidal creek bank. Geochim Cosmochim Acta 140:418–434. https://doi.org/10.1016/j.gca.2014.05.038

Senesi N (1992) Binding mechanisms of pesticides to soil humic substances. Sci Total Environ 123–124:63–76. https://doi.org/10.1016/0048-9697(92)90133-D

Serelis K, Mantzos N, Meintani D, Konstantinou I (2021) The effect of biochar, hydrochar particles and dissolved organic matter on the photodegradation of metribuzin herbicide in aquatic media. J Environ Chem Eng 9:105027. https://doi.org/10.1016/j.jece.2021.105027

Shank GC, Evans A, Yamashita Y, Jaffé R (2011) Solar radiation–enhanced dissolution of particulate organic matter from coastal marine sediments. Limnol Oceanogr 56:577–588. https://doi.org/10.4319/lo.2011.56.2.0577

Shi Q, Zhang Y, Chung KH, Zhao S, Xu C (2021) Molecular characterization of fossil and alternative fuels using electrospray ionization fourier transform ion cyclotron resonance mass spectrometry: recent advances and perspectives. Energy Fuels 32(22):18019–18055. https://doi.org/10.1021/acs.energyfuels.1c01671

Sleighter RL, Hatcher PG (2007) The application of electrospray ionization coupled to ultrahigh resolution mass spectrometry for the molecular characterization of natural organic matter. J Mass Spectrom 42:559–574. https://doi.org/10.1002/jms.1221

Smith CR, Buzan EM, Lee JW (2013) Potential impact of biochar water-extractable substances on environmental sustainability. Acs Sustainable Chemistry & Engineering 1:118–126. https://doi.org/10.1021/sc300063f

Song B, Chen M, Zhao L, Qiu H, Cao X (2019) Physicochemical property and colloidal stability of micron- and nano-particle biochar derived from a variety of feedstock sources. Sci Total Environ 661:685–695. https://doi.org/10.1016/j.scitotenv.2019.01.193

Stenson AC, Marshall AG, Cooper WT (2003) Exact masses and chemical formulas of individual suwannee river fulvic acids from ultrahigh resolution electrospray ionization fourier transform ion cyclotron resonance mass spectra. Anal Chem 75:1275–1284. https://doi.org/10.1021/ac026106p

Stubbins A, Spencer RGM, Chen H, Hatcher PG, Mopper K, Hernes PJ, Mwamba VL, Mangangu AM, Wabakanghanzi JN, Six J (2010) Illuminated darkness: Molecular signatures of Congo River dissolved organic matter and its photochemical alteration as revealed by ultrahigh precision mass spectrometry. Limnol Oceanogr 55:1467–1477. https://doi.org/10.4319/lo.2010.55.4.1467

Stubbins A, Spencer R G M, Mann P J, Holmes R M, McClelland J W, Niggemann J, Dittmar T (2015) Utilizing colored dissolved organic matter to derive dissolved black carbon export by arctic rivers. 3. https://doi.org/10.3389/feart.2015.00063

Stubbins A, Hood E, Raymond PA, Aiken GR, Sleighter RL, Hernes PJ, Butman D, Hatcher PG, Striegl RG, Schuster P, Abdulla HAN, Vermilyea AW, Scott DT, Spencer RGM (2012a) Anthropogenic aerosols as a source of ancient dissolved organic matter in glaciers. Nat Geosci 5:198–201. https://doi.org/10.1038/ngeo1403

Stubbins A, Niggemann J, Dittmar T (2012b) Photo-lability of deep ocean dissolved black carbon. Biogeosciences 9:1661–1670. https://doi.org/10.5194/bg-9-1661-2012

Tang J, Li X, Luo Y, Li G, Khan S (2016) Spectroscopic characterization of dissolved organic matter derived from different biochars and their polycyclic aromatic hydrocarbons (PAHs) binding affinity. Chemosphere 152:399–406. https://doi.org/10.1016/j.chemosphere.2016.03.016

Tian Y, Feng L, Wang C, Liu Y, Zou J, Li R, Du Z, Zhang L (2019) Dissolved black carbon enhanced the aquatic photo-transformation of chlortetracycline via triplet excited-state species: The role of chemical composition. Environ Res 179:108855. https://doi.org/10.1016/j.envres.2019.108855

Vetere A, Schrader W (2017) Mass spectrometric coverage of complex mixtures – exploring the carbon space of crude oil. ChemistrySelect 2:849–853. https://doi.org/10.1002/slct.201601083

Chen *et al. Carbon Research*   (2022) 1:23

Page 19 of 19

Wagner S, Jaffé R (2015) Effect of photodegradation on molecular size distribution and quality of dissolved black carbon. Org Geochem 86:1–4. https://doi.org/10.1016/j.orggeochem.2015.05.005

Wagner S, Riedel T, Niggemann J, Vähätalo AV, Dittmar T, Jaffé R (2015) Linking the molecular signature of heteroatomic dissolved organic matter to watershed characteristics in world rivers. Environ Sci Technol 49:13798–13806. https://doi.org/10.1021/acs.est.5b00525

Wagner S, Jaffé R, Stubbins A (2018) Dissolved black carbon in aquatic ecosystems. Limnology and Oceanography Letters 3:168–185. https://doi.org/10.1002/lol2.10076

Wagner S, Brandes J, Spencer RGM, Ma K, Rosengard SZ, Moura JMS, Stubbins A (2019) Isotopic composition of oceanic dissolved black carbon reveals non-riverine source. Nat Commun 10:5064. https://doi.org/10.1038/s41467-019-13111-7

Wan D, Wang J, Dionysiou DD, Kong Y, Yao W, Selvinsimpson S, Chen Y (2021) Photogeneration of reactive species from biochar-derived dissolved black barbon for the degradation of amine and phenolic pollutants. Environ Sci Technol 55:8866–8876. https://doi.org/10.1021/acs.est.1c01942

Wang D, Zhang W, Hao X, Zhou D (2013) Transport of biochar particles in saturated granular media: effects of pyrolysis temperature and particle size. Environ Sci Technol 47:821–828. https://doi.org/10.1021/es303794d

Wang X, Xu C, Druffel EM, Xue Y, Qi Y (2016) Two black carbon pools transported by the Changjiang and Huanghe Rivers in China. Global Biogeochem Cycles 30:1778–1790. https://doi.org/10.1002/2016GB005509

Wang H, Zhou H, Ma J, Nie J, Yan S, Song W (2020) Triplet photochemistry of dissolved black carbon and its effects on the photochemical formation of reactive oxygen species. Environ Sci Technol 54:4903–4911. https://doi.org/10.1021/acs.est.0c00061

Wang K, Zhang Y, Sun B, Yang Y, Xiao B, Zhu L (2021) New insights into the enhanced transport of uncoated and polyvinylpyrrolidone-coated silver nanoparticles in saturated porous media by dissolved black carbons. Chemosphere 283:131159. https://doi.org/10.1016/j.chemosphere.2021.131159

Ward CP, Sleighter RL, Hatcher PG, Cory RM (2014) Insights into the complete and partial photooxidation of black carbon in surface waters. Environmental Science-Processes & Impacts 16:721–731. https://doi.org/10.1039/c3em00597f

Wei CH, Fu HY, Qu XL, Zhu DQ (2017) Environmental processes of dissolved black carbon. Progress in Chemistry 29:1042–1052. https://doi.org/10.7536/pc170444

Weishaar JL, Aiken GR, Bergamaschi BA, Fram MS, Fujii R, Mopper K (2003) Evaluation of specific ultraviolet absorbance as an indicator of the chemical composition and reactivity of dissolved organic carbon. Environ Sci Technol 37:4702–4708. https://doi.org/10.1021/es030360x

Wenk J, von Gunten U, Canonica S (2011) Effect of dissolved organic matter on the transformation of contaminants induced by excited triplet states and the hydroxyl radical. Environ Sci Technol 45:1334–1340. https://doi.org/10.1021/es102212t

Woods GC, Simpson MJ, Kelleher BP, McCaul M, Kingery WL, Simpson AJ (2010) Online high-performance size exclusion chromatography—nuclear magnetic resonance for the characterization of dissolved organic matter. Environ Sci Technol 44:624–630. https://doi.org/10.1021/es903042s

Woolf D, Amonette JE, Street-Perrott FA, Lehmann J, Joseph S (2010) Sustainable biochar to mitigate global climate change. Nat Commun 1:56. https://doi.org/10.1038/ncomms1053

Wozniak AS, Goranov AI, Mitra S, Bostick KW, Zimmerman AR, Schlesinger DR, Myneni S, Hatcher PG (2020) Molecular heterogeneity in pyrogenic dissolved organic matter from a thermal series of oak and grass chars. Org Geochem 148:104065. https://doi.org/10.1016/j.orggeochem.2020.104065

Wu J, Zhang H, He P-J, Shao L-M (2011) Insight into the heavy metal binding potential of dissolved organic matter in MSW leachate using EEM quenching combined with PARAFAC analysis. Water Res 45:1711–1719. https://doi.org/10.1016/j.watres.2010.11.022

Xia K, Bleam W, Helmke PA (1997) Studies of the nature of Cu2+ and Pb2+ binding sites in soil humic substances using X-ray absorption spectroscopy. Geochim Cosmochim Acta 61:2211–2221. https://doi.org/10.1016/S0016-7037(97)00079-3

Xu C, Xue Y, Qi Y, Wang X (2016) Quantities and fluxes of dissolved and particulate black carbon in the changjiang and huanghe Rivers, China. Estuaries Coasts 39:1617–1625. https://doi.org/10.1007/s12237-016-0122-0

Xu Y, Ou Q, Liu C, Zhou X, He Q, Wu Z, Huang R, Ma J, Lu D, Huangfu X (2020) Aggregation and deposition behaviors of dissolved black carbon with coexisting heavy metals in aquatic solution. Environ Sci Nano 7:2773–2784. https://doi.org/10.1039/D0EN00373E

Xu Y, Ou Q, He Q, Wu Z, Ma J, Huangfu X (2021) Influence of dissolved black carbon on the aggregation and deposition of polystyrene nanoplastics: Comparison with dissolved humic acid. Water Res 196:117054. https://doi.org/10.1016/j.watres.2021.117054

Yamamoto H, Liljestrand HM, Shimizu Y, Morita M (2003) Effects of physical—chemical characteristics on the sorption of selected endocrine disruptors by dissolved organic matter surrogates. Environ Sci Technol 37:2646–2657. https://doi.org/10.1021/es026405w

Yamashita Y, Kojima D, Yoshida N, Shibata H (2021) Relationships between dissolved black carbon and dissolved organic matter in streams. Chemosphere 271:129824. https://doi.org/10.1016/j.chemosphere.2021.129824

Yan W, Chen Y, Han L, Sun K, Song F, Yang Y, Sun H (2022) Pyrogenic dissolved organic matter produced at higher temperature is more photoactive: Insight into molecular changes and reactive oxygen species generation. J Hazard Mater 425:127817. https://doi.org/10.1016/j.jhazmat.2021.127817

Zencak Z, Elmquist M, Gustafsson Ö (2007) Quantification and radiocarbon source apportionment of black carbon in atmospheric aerosols using the CTO-375 method. Atmos Environ 41:7895–7906. https://doi.org/10.1016/j.atmosenv.2007.06.006

Zhang P, Huang P, Xu X, Sun H, Jiang B, Liao Y (2020a) Spectroscopic and molecular characterization of biochar-derived dissolved organic matter and the associations with soil microbial responses. Sci Total Environ 708:134619. https://doi.org/10.1016/j.scitotenv.2019.134619

Zhang P, Shao Y, Xu X, Huang P, Sun H (2020b) Phototransformation of biochar-derived dissolved organic matter and the effects on photodegradation of imidacloprid in aqueous solution under ultraviolet light. Sci Total Environ 724:137913. https://doi.org/10.1016/j.scitotenv.2020.137913

Zhang R, Sun B, Song Y, Chen X, Song C, Wei Z, Su X, Zhang C, Wu Z (2021a) Evaluating the phytotoxicity of dissolved organic matter derived from black carbon. Sci Total Environ 778:146231. https://doi.org/10.1016/j.scitotenv.2021.146231

Zhang X, Chen Z, Huo X, Kang J, Zhao S, Peng Y, Deng F, Shen J, Chu W (2021) Application of Fourier transform ion cyclotron resonance mass spectrometry in deciphering molecular composition of soil organic matter: a review. Sci Total Environ 756:144140

Zhong D, Zhao Z, Jiang Y, Yang X, Wang L, Chen J, Guan C-Y, Zhang Y, Tsang DCW, Crittenden JC (2020) Contrasting abiotic As(III) immobilization by undissolved and dissolved fractions of biochar in Ca2+-rich groundwater under anoxic conditions. Water Res 183:116106. https://doi.org/10.1016/j.watres.2020.116106

Zhou H, Lian L, Yan S, Song W (2017) Insights into the photo-induced formation of reactive intermediates from effluent organic matter: The role of chemical constituents. Water Res 112:120–128. https://doi.org/10.1016/j.watres.2017.01.048

Zhou Z, Chen B, Qu X, Fu H, Zhu D (2018) Dissolved Black Carbon as an Efficient Sensitizer in the Photochemical Transformation of 17β-Estradiol in Aqueous Solution. Environ Sci Technol 52:10391–10399. https://doi.org/10.1021/acs.est.8b01928

Zhou L, Zhou Y, Tang X, Zhang Y, Jang K-S, Székely AJ, Jeppesen E (2021) Resource aromaticity affects bacterial community successions in response to different sources of dissolved organic matter. Water Res 190:116776. https://doi.org/10.1016/j.watres.2020.116776

Zhu S, Zhao W, Wang P, Zhao L, Jin C, Qiu R (2021) Co-transport and retention of zwitterionic ciprofloxacin with nano-biochar in saturated porous media: Impact of oxidized aging. Sci Total Environ 779:146417. https://doi.org/10.1016/j.scitotenv.2021.146417

Ziolkowski LA, Chamberlin AR, Greaves J, Druffel ERM (2011) Quantification of black carbon in marine systems using the benzene polycarboxylic acid method: a mechanistic and yield study. Limnol Oceanogr Methods 9:140–140. https://doi.org/10.4319/lom.2011.9.140

Publisher's Note